



# **Università degli Studi di Milano**

Doctorate School of Chemical Sciences and Technologies

Ph.D. in Industrial Chemistry  
XXIV Cycle

## **Study of physico-chemical parameters characterizing naphthenic acid corrosion**

Candidate: Maria Elena Gennaro R08291

Advisor: Dr. Stefano P. M. Trasatti  
Co-advisor: Marco Scapin  
Coordinator: Prof. Dominique Roberto



## Index

1. Introduction .....	5
1.1. Naphthenic Acid structure and chemistry .....	5
1.2. Naphthenic Acid corrosion .....	6
1.3. Naphthenic Acids characterization .....	11
1.4. Testing equipment .....	14
2. Experimental .....	17
2.1. Analytical characterization .....	17
2.2. Materials .....	19
2.3. Testing environment .....	19
2.4. Corrosion tests equipment .....	23
2.5. Corrosion rate evaluation .....	29
2.6. Experimental design .....	29
3. HT – HP testing .....	33
3.1. Results and discussion .....	33
3.2. Remarks .....	40
4. Small plant for crude corrosivity .....	41
4.1. Plant validation .....	41
4.2. Tests with crudes .....	45
4.3. 3 <sup>2</sup> factorial plan results and analysis .....	48
4.4. Tests with natural acidic crude oils .....	63
4.5. Discussion .....	65

## List of tables

Table 1.1 – ESI MS/MS analysis of standard acids .....	12
Table 2.1 – Spectral ranges of <sup>1</sup> H and <sup>13</sup> C NMR signals of NAs and main observed functionalities.....	18
Table 2.2 – Compositions of the steels employed for the experimental activity ....	19
Table 2.3 – Main properties of the gasoil used for tests.....	19
Table 2.4 – Gasoil cut points.....	20
Table 2.5 – Molar % distributions of H and C in NAs .....	22
Table 2.6 – Molar % distribution of primary and secondary acids .....	23
Table 2.7 – Main characteristics of the crude used in corrosion tests.....	23
Table 2.8 – Specimen geometry for HT-HP tests.....	24
Table 2.9 – HT-HP test matrix.....	26
Table 2.10 – 3 <sup>2</sup> Full factorial plan.....	30
Table 2.11 – Factors and levels for the experimental plan .....	30
Table 3.1 – HT- HP tests results and crudes analyses.....	34
Table 3.2 – Calculated H <sub>2</sub> S and NAs contributions to corrosion rate (A data are reported for comparison .....	37
Table 4.1 – Tests with gasoil and NA commercial mixture .....	42
Table 4.2 – Test matrix and results for tests wth low sulphur crude .....	46
Table 4.3 – Test results for high sulphur crude at 350° C .....	46
Table 4.4 – Comparison of experimental corrosion rates and values from modified McConomy curves.....	47
Table 4.5 – Test matrix and results for the experimental plan .....	48
Table 4.6 – ANOVA table of the complete model for ln(CS CR).....	51
Table 4.7 – ANOVA table for the simplified model.....	52
Table 4.8 – Coefficients of the model for ln(CS CR) .....	57
Table 4.9 – ANOVA table of the complete model for 5Cr CR .....	59
Table 4.10 – ANOVA table of the simplified model for 5Cr CR.....	60
Table 4.11 –Coefficients of the model for 5Cr CR .....	63
Table 4.12 – Test matrix and results for acid crudes.....	64

## List of figures

Figure 1.1 – Examples of naphthenic acids molecules with different hydrogen deficiency (Z) values .....	6
Figure 1.2 – Main areas subjected to naphthenic acids attack in refinery crude units.....	7
Figure 1.3 – Hypothesis for the mechanism of assistance and/or passivation of NA corrosion.....	10
Figure 1.4 – ESI (-) mass spectra of some acids.....	13
Figure 1.5 – Example of FTIR spectrum of an acid mixture extracted from a crude .....	13
Figure 1.6 – Example of a plant for tests with rotating cylinder <sup>24</sup> .....	15
Figure 2.1 – ESI (-) spectrum of the NA commercial mixture used in the tests ....	21
Figure 2.2 – NMR spectra of the NA commercial mixture. (A) <sup>1</sup> H; (B) <sup>13</sup> C .....	21
Figure 2.3 – <sup>13</sup> C spectrum of the carboxylic groups: mainly primary acids are evident.....	22
Figure 2.4 – HT-HP testing configuration.....	25
Figure 2.5 – HT-HP specimen mounted in the autoclave .....	25
Figure 2.6 – Small plant to determine crude corrosivity.....	27
Figure 2.7 – Specimen geometry and appearance.....	27
Figure 2.8 – Incident flow specimen holder (left); tangential flow specimen holder (right).....	28
Figure 3.1 – Pressure increase during a three days test with A oil .....	35
Figure 3.2 – Corrosion rate of A, B and Coils vs. TAN and S content.....	36
Figure 3.3 – API 5L X65 carbon steel specimens after 3 days tests in A oil, without degassing, at 270°C (on the left) and 350°C (on the right).....	37
Figure 3.4 – API 5L X65 specimens after 1 day (on the left) and 3 days (on the right) tests in A oil, at 350°C, with autoclave degassing .....	38
Figure 3.5 – 5Cr specimens after 1 day (on the left) and 3 days (on the right) tests in A oil, at 350°C, with autoclave degassing .....	38
Figure 3.6 – 5Cr specimens after 1 day (on the left) and 3 days (on the right) tests in C oil, at 350°C, with autoclave degassing .....	39
Figure 3.7 – 5Cr specimens after 1 day (on the left) and 3days (on the right) tests	

in B oil, at 350°C, with autoclave degassing .....	39
Figure 4.1 – Corrosion rate vs. TAN; test conducted on 5Cr for 24 hours at 330°C; incident flow, 0.4 m/s .....	43
Figure 4.2 – Corrosion rate vs. flow velocity; test conducted at TAN 4, 330°C, for 24 hours; tangential flow.....	43
Figure 4.3 – TAN trend with test duration at 350°C.....	44
Figure 4.4 – ESI(-)-MS spectra of the extracted acids from a mixture gasoil-NA at initial TAN 2: (a) initial; (B) after 3 days of test; (C) after 8 days of test.....	45
Figure 4.5 – Modified McConomy curves .....	47
Figure 4.6 – Appearance of CS coupon after treatment n.13 .....	49
Figure 4.7 – Appearance of 5Cr steel after treatment n.13.....	49
Figure 4.8 – Box-plot, histograms and normal probability plot for CS CR variable .....	50
Figure 4.9 – Hystograms, box-plot and normal probability plot for transformed variable $\ln(\text{CS CR})$ .....	50
Figure 4.10 – Half-normal probability plot of the effects for $\ln(\text{CS CR})$ .....	52
Figure 4.11 – Box plot, histograms and normal probability plot of residuals for $\ln(\text{CS CR})$ variable.....	53
Figure 4.12 – Residuals vs. observed (left) and predicted (right) values .....	54
Figure 4.13 – Residuals vs. case number.....	54
Figure 4.14 – Predicted vs. observed vlues for $\ln(\text{CS CR})$ .....	55
Figure 4.15 – Response surface for $\ln(\text{CS CR})$ .....	56
Figure 4.16 – Contour plot for $\ln(\text{CS CR})$ .....	56
Figure 4.17 – Box-plot, histograms and normal probability plot for 5Cr CR .....	58
Figure 4.18 – Box-plot of response variable for TAN (left) and Sulphur (right) .....	59
Figure 4.19 – Box-plot, histograms and normal probability plot of residuals for 5Cr CR .....	61
Figure 4.20 – Residuals vs. observed (left) and predicted values (right) .....	61
Figure 4.21 – Residuals vs. case number.....	62
Figure 4.22 – Response surface for 5Cr CR.....	62
Figure 4.23 – Contour plot for 5Cr CR.....	63
Figure 4.24 – Surface appearance of 5Cr steel coupon after the test (left) and then	

after pickling (right).....	64
Figure 4.25 – Surface appearance of CS coupon after the test (left) and then after pickling (right).....	65
Figure 4.26 – Corrosion mechanisms and environment composition for 5Cr steel	66
Figure 4.27 – Corrosion mechanisms and environment composition for CS.....	66
Figure 4.28 – NA distribution in crude F vs. number of C atoms (left) and of rings(right) .....	67









## Abstract

The recent increase in crude oil cost arose interest in cheaper oils, usually called “opportunity crudes”. These oils are difficult to transport and treat, mainly because of their sulphur content, acidity and high density, but their cheap price makes them attractive, because refineries capable of processing them could gain a higher profit. Opportunity crudes composition affects process parameters and they can also cause corrosion and failures in plant equipment.

It is well known that the main corrosive agents are the naphthenic acids (NAs), but the mechanism is complex and very little is known about it since there are many factors affecting it such as type of acids, temperature, sulphur compounds and fluid velocity.

Thus damage process has not been clarified yet and at this time there is no accurate model available for predicting crude oil corrosiveness.

Though considerable work has been done to understand NA corrosion in refineries, it turned out to be unsuccessful when the interdependence of NAs type and corrosion effects is considered.

The objective of the research activity was to get more insight into the relationships between physico-chemical properties of crude oils and corrosion, in order to build a model aimed at identification of a corrosivity index which might help operators to determine the aggressiveness of processed fluids.

For this purpose an analytical protocol was identified in order to determine the main molecular characteristics, such as number of carbon atoms, rings and average molecular weight. After some preliminary high temperature and pressure tests, a new equipment was developed and designed capable of reproducing real plant conditions. The small-scale plant was first used with a reference fluid consisting of gasoil and a commercial mixture of NAs, and then tested with actual crudes. The use of experimental design and of proper analytical techniques allowed to build a model for the corrosion of two different materials.



---

## **Acknowledgements**

I would like to thank my advisors Dr. Stefano P.M. Trasatti and Dr. Marco Scapin for their support during these years. I would also like to thank my company Venezia Tecnologie SpA, that gave me the opportunity to study again and to carry out this project.

I would like to acknowledge the financial support of eni R&M that financed this research project.

I would like to express my gratitude to my colleagues, Marino Tolomio, Sergio Sgorlon and Alberto Pontarollo, for their patience and technical and moral support during all the research project. Thank also to Romeo Menegazzo, for his clever contributions to the technical development.

I would also like to thank Luciano Montanari and Cristina Flego in eni R&M SDM CHIF laboratories, for providing all the support for the analyses and their interpretation.

A special thanks to my husband, Marco, for his patience and continuous support, to little Alice, for her unconscious patience and to my family, who always encouraged me.



# 1. Introduction

## 1.1. Naphthenic Acid structure and chemistry

The term “naphthenic acids” is actually used to address all carboxylic acids found in hydrocarbon reservoirs, including acyclic and aromatic ones.

Naphthenic acids are found in naturally biodegraded oils from eastern Europe, Russia, California and Venezuela, and they are considered as a biological marker strictly connected to the maturity and biodegradation of the field<sup>1</sup>.

NAs are usually in oils which didn't undergo sufficient catagenesis or were biodegraded by bacteria. Usually heavy oils coming from young reservoirs have the highest acid content whereas paraffinic oils have a lower content<sup>2</sup>.

NA content is expressed using Total Acid Number (TAN) which expresses KOH milligrams necessary to neutralise one gram of oil<sup>3,4</sup>. However TAN characterizes a general acidity (i.e. phenols, mercaptans, aromatic acids, thiophenes, pyrroles) not only the naphthenic one<sup>5,6</sup>.

Naphthenic acids are classified as carboxylic acids having one or more cycloalkane rings (naphthenes) with the general formula  $C_nH_{2n+Z}O_2$ <sup>1,7,8</sup> where Z is hydrogen deficiency which can be zero or an even negative number that specifies a homologous series. Actually Z can be considered as an index for the number of double bonds and rings in the molecule, so more structures correspond to a given Z number (see Figure 1.1)<sup>9</sup>.

Their molecular weight can range among different values and both small and very large molecules can be found. Polarity and non-volatility of naphthenic acids

increase as the molecular weight increases, hence compounds can exhibit different physical, chemical and toxicological properties<sup>10</sup>.

They are completely soluble in organic solvents, whereas the solubility in water depends on pH value; pKa ranges between 5 and 6<sup>11,12</sup>.

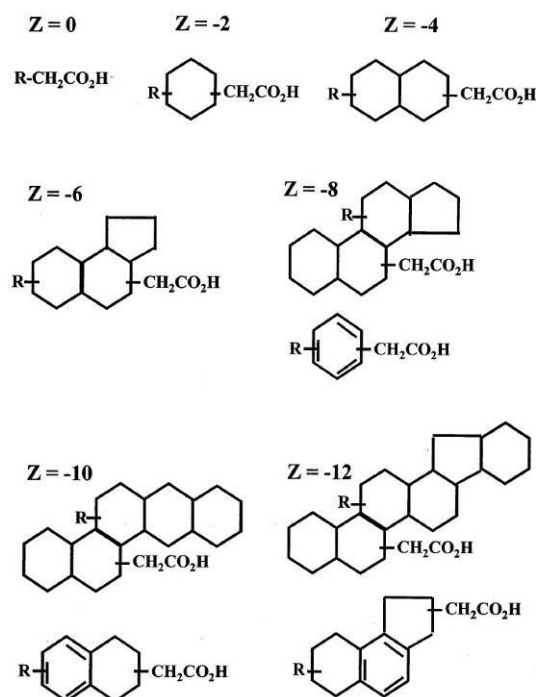
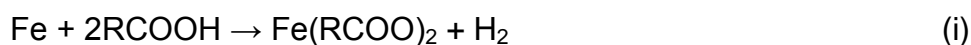


Figure 1.1 – Examples of naphthenic acids molecules with different hydrogen deficiency (Z) values

## 1.2. Naphthenic Acid corrosion

NA corrosion usually occurs in crude distillation units at temperatures between 200 and 400 °C, damaging heating tubes in furnaces, elbows, transfer lines and vacuum areas (see Figure 1.2)<sup>13</sup>.

The corrosion mechanism of NA attack takes into consideration also the presence of sulphur compounds, which can inhibit or accelerate the phenomenon, even if it is not known to which extent. The main accepted mechanism is described by the following reactions<sup>6</sup>:



According to reactions *i* to *iii*, NAs react with iron on the metal surface, generating



iron naphthenates which are soluble in the oil phase. At the same time hydrogen sulphide can produce an insoluble iron sulphide film on the metal surface. Piehl<sup>14</sup> said that these two processes compete with each other and one reaction can take place retarding the other one. Hydrogen sulphide can also react with iron naphthenate, regenerating NAs.

It is not clear yet if the mechanism acting is a chemical or electrochemical one; in fact conductivity measurements carried out on crudes produced very low values, which exclude electrochemical phenomena<sup>6</sup>. However Zheng et al.<sup>15,16</sup> stated that at high temperatures NAs can dissociate activating another mechanism different from the one operating at lower temperatures. This seems to be confirmed by the corrosion morphology which becomes more selective with the increase of temperature.

Parameters affecting corrosiveness that were studied during recent years are acidity, interaction with sulphur compounds and flow velocity<sup>17</sup>.

#### *Acidity*

As reported above, usually NA content is measured by TAN value. However this parameter cannot be a reliable index of a crude's corrosiveness, in fact in some cases corrosion rate increases with total acidity<sup>18,19,20</sup> whereas in others no clear dependence is observed<sup>21,22,23</sup>.

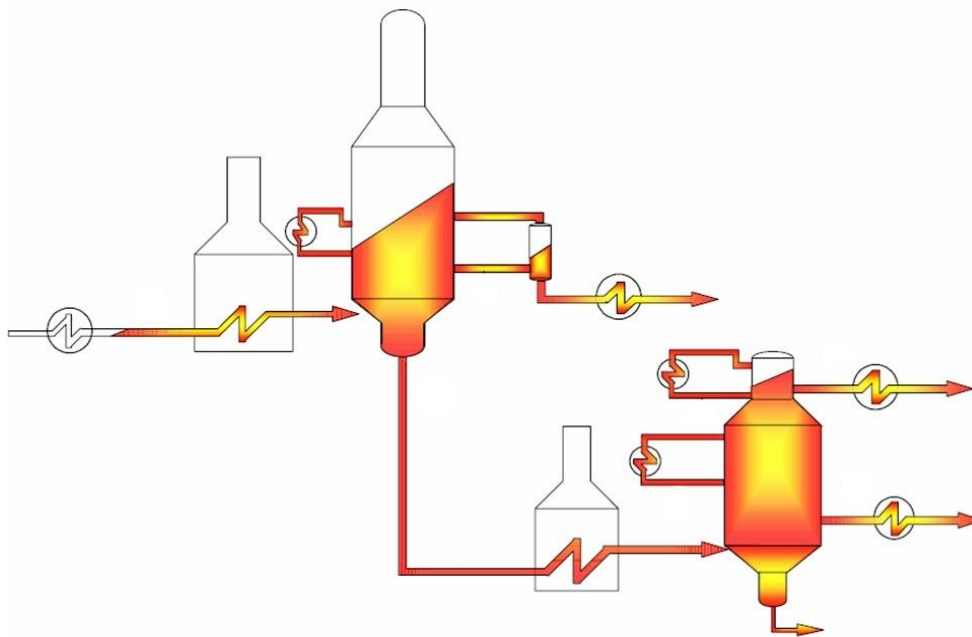


Figure 1.2 – Main areas subjected to naphthenic acids attack in refinery crude units

---

It seems that the real important parameter is the nature of the acid mixture present in the crudes together with molecular structure, polarity and distribution as a function of temperature of single acidic species: these characteristics affect reactivity thus aggressiveness towards the metal surface<sup>6,24</sup>.

This opinion appears now to be generally accepted and some tentative researches were carried out in order to correlate corrosiveness and composition analyses<sup>18,20,22,25,26</sup>.

Slavcheva *et al.*<sup>27</sup> conducted experiments with a group of NAs with different carbon numbers, boiling points and the same TAN value. The composition of these oils was analysed by fast atom bombardment mass spectroscopy (FAB-MS). It was observed that the number of  $(CH_2)_n$  groups present in the oil plays a key role in NA corrosion. The corrosion rate by NAs increased with an increase of  $(CH_2)_n$  groups up to  $n = 3$ . Slavcheva *et al.* suggested that at higher values of  $n$ , adsorption of acid molecules was retarded by the steric hindrance between the long carbon chains, and thus the corrosion rate decreased.

On the basis of field experience some theories have been developed that accounts for type  $\alpha$ , "bad" acids and type  $\beta$ , "good" ones, depending on their molecular weight; moreover it seems that above a certain value of molecular weight acids can act as corrosion inhibitors<sup>28</sup>. The methodology that consists in feeding a plant by blending proper quantities of crudes containing  $\alpha$  and  $\beta$  acids was also patented twice<sup>29</sup>.

Results are, however, not exhaustive, since analysis procedures have not been validated yet and they need further studies. Moreover a model capable of relating molecular characteristics and corrosiveness is not available.

Despite the inconsistencies about TAN value and corrosivity, this parameter is still used to estimate crude oil aggressiveness. Hence crudes with a TAN lower than 0.5 are considered to be non corrosive whereas fraction with TAN higher than 1.5 are believed to be aggressive<sup>30,31</sup>.

### *Influence of sulphur compounds*

The presence of sulphur compounds is a key factor in corrosion phenomena taking place in crude distillation units. In fact, it is well known that at high temperature some compounds decompose and produce  $H_2S$ .

Hydrogen sulphide reacts with iron producing iron sulphide (FeS from high temperature sulphidation); this high temperature corrosion is usually observed in process units at temperatures above  $260\text{ }^\circ\text{C}$ <sup>32</sup>, the layer that grows on the metal surface is sometimes protective and this is very important in NA corrosion.

Both in the laboratory and in the field it was observed that metal surfaces were covered with a film of some sort<sup>31,33</sup>. This macroscopic film was mainly composed

of metal sulphides, and was called “pseudo-passive film” since it was supposed to protect metals from the attack of NAs to some extent. The pseudo-passive film had great influence on the synergism of acid attack and sulphidation. It was found that at least three kinds of interactive corrosion could take place:

1. NA corrosion with a very thin film of corrosion products;
2. Sulphidation corrosion accelerated by NA attack;
3. NA corrosion partially inhibited by sulphidation.

Bota et al.<sup>34</sup> verified that there is no obvious correlation between the iron sulfide scale thickness/morphology and the protection provided to mitigate naphthenic acid corrosion.

Jet-impingement tests have been conducted on pre-sulphided specimens with transformer oil and a commercial mixture of NAs. These tests showed that the produced damage was affected by acid concentration beside flow velocity: in fact, high TAN values can dissolve sulphide layer exposing the bare metal.

Nonetheless at intermediate H<sub>2</sub>S partial pressures, iron sulphide layer is protective whereas at higher H<sub>2</sub>S contents sulphidation occurs that is accelerated by high flow velocity<sup>16,28,35</sup>.

Tests carried out with iron powder proved that during high temperature treatment H<sub>2</sub>S evolution depends on the particular compound and can affect the corrosion phenomena. In particular compounds which have higher boiling temperature, i.e. thermally more stable such as thiophenes, are less subjected to decomposition and H<sub>2</sub>S evolution than mercaptans and sulphides.

Yépez proposed an interesting description about possible mechanisms involving different sulphur compounds, such as hydrogen sulphide, mercaptans, sulphides, thiophenes, sulphones and sulphoxides.

Reactions (i)-(iii) compete with each other and depending on species concentration one can overcome the others:

- *H<sub>2</sub>S*: it acts as an inhibitor for concentrations above 7.5% (ii overcomes i)
- *Mercaptans*: they need to be reduced to H<sub>2</sub>S to be active towards reactions (i)-(iii), hence they need hydrogen. Inhibitive effect is clear above 220°C.
- *Sulphides*: they behave in a similar way as mercaptans, but they are more efficient inhibitors, probably because their molecules contain more sulphur.
- *Thiophenes and sulphones*: they have no effect, because at these temperatures they do not undergo reduction and do not produce H<sub>2</sub>S.
- *Sulphoxides*: they promote NA corrosion: indeed the measured dissolved iron is higher than with acids alone. The cause is water production due to their reduction according to the following reaction:

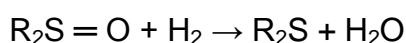


Figure 1.3 shows one possible mechanism.

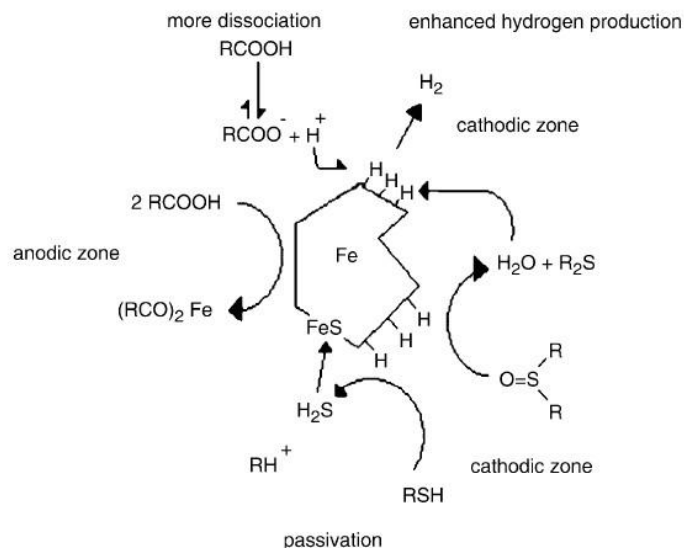


Figure 1.3 – Hypothesis for the mechanism of assistance and/or passivation of NA corrosion

In summary sulphur compounds affect NA corrosion insofar as protons produced by the corrosive process reduce them. When the product of reduction is  $H_2S$ , iron sulphide formation can prevent a further attack to the material. When the product is  $H_2O$ , a further acid dissociation becomes possible that fosters cathodic process hence the global corrosion phenomenon<sup>36</sup>.

In refinery plants, however, these differences are not taken into account and the blends of processed feeds are designed on the basis of total sulphur content.

### *Flow velocity*

It is well known that high flow velocities worsen NA corrosion. In fact, there is a synergic effect due to higher mass transport, stronger erosion (higher shear stresses) and fast desorption/dissolution of corrosion products.

Usually the highest velocities occur in transfer lines and can reach values of 40-50 m/s<sup>37,38</sup>.

Many studies have been conducted both in laboratories and in the field. Each time higher corrosion rates are reported than those measured in static conditions<sup>16,24,39</sup>; as an example jet impingement tests with shear stresses of about 5000 N/m<sup>2</sup> produced corrosion rate forty times higher than in static conditions.

### *Materials*

Refinery experience shows as carbon steel is not enough resistant to NA attack, nor to high temperature sulphidation. As a first solution austenitic stainless steels such as low alloyed as 5Cr and 9Cr or AISI 316 and 317 have been employed; if also these materials are subjected to failure, the use of an alloy with a minimum molybdenum content of 2.5% is suggested<sup>40</sup>.

The presence of chromium allows the formation of mixed sulphides that are more stable and protective than FeS alone, whereas the beneficial function of molybdenum is attributed to its low affinity towards RCOO<sup>-</sup> radical, the improvement of the superficial film, that provides a better resistance to pitting and enhanced microstructure and microhardness that allow lower erosion<sup>15</sup>.

### **1.3. Naphthenic Acids characterization**

As reported above, usually NA content is measured by TAN value. Two standard tests are conventionally used to measure TAN, namely ASTM D974 and ASTM D664. ASTM D974 is a colorimetric method based on colour change of indicator with addition of KOH. ASTM D664 is a potentiometric method based on change in electrical conductivity of the sample by addition of KOH. These two methods are not completely accurate, as the TAN determined accounts for not only the presence of NAs but also inorganic acids, phenolic compounds, mercaptans and salts.

Despite the huge work done to develop an effective and reliable procedure capable of characterizing these compounds, the issue has not been solved yet.

Indeed, it is very difficult to isolate single acidic species and the complete separation, quantification and identification of the compounds has not been accomplished yet, due to the complexity of NA mixtures which exhibit variations in structure and molecular weight. Several analytical techniques have been utilized to characterize the acids qualitatively. Most work has been focused on major spectrometric techniques such as mass, infrared and nuclear magnetic resonance spectroscopy.

Mass spectrometry has been widely employed to analyse acidic species in crude oils after extraction and/or derivatization. Esters derivatized from acids were analysed by GC-MS<sup>1</sup>; nonetheless it is preferable to directly analyse acidic species, as derivatization could cause loss of material and information. Thus different ionization methods have been studied such as Fast Atom Bombardment (FAB), Atmospheric Pressure Chemical Ionization (APCI) and Electro-Spray Ionization (ESI).

FAB-MS impacts molecules in a hard way, so lighter techniques are more suitable<sup>18</sup>. ESI-MS and APCI-MS showed better results in negative ion mode, in particular ESI-MS exhibited higher intensities and is the most used technique (see Figure 1.4). Table 1.1 shows the position of typical acid peaks<sup>9</sup>.

Recently also “ultra high” resolution techniques such as FTICR-MS have been employed<sup>41,42,43</sup>.

Table 1.1 – ESI MS/MS analysis of standard acids

Compound	Parent m/z [M-H] <sup>-</sup>	Daughter (m/z) <sup>a</sup>	Mass loss	Neutral loss fragment
cyclohexylacetic acid	141	97	44	CO <sub>2</sub>
cyclohexanebutyric acid	169	125, 151	44, 18	CO <sub>2</sub> , H <sub>2</sub> O
adamantaneacetic acid	193	149, 175, 165	44, 18, 28	CO <sub>2</sub> , H <sub>2</sub> O, CO
5 $\alpha$ -cholanic acid	359	341, 331, 315	18, 28, 44	H <sub>2</sub> O, CO, CO <sub>2</sub>
2-naphthylacetic acid	185	141, 157	44, 28	CO <sub>2</sub> , CO
1,2,3,4-tetrahydronaphthoic acid	175	131, 147, 157	44, 28, 18	CO <sub>2</sub> , CO, H <sub>2</sub> O
benzoic acid	121	77	44	CO <sub>2</sub>
1-pyreneboxylic acid	245	201	44	CO <sub>2</sub>
1-pyreneacetic acid	259	215	44	CO <sub>2</sub>
1-pyrenebutyric acid	287	215	72	CO <sub>2</sub> + C <sub>2</sub> H <sub>2</sub>

<sup>a</sup> Daughter peaks listed in order of relative abundance.

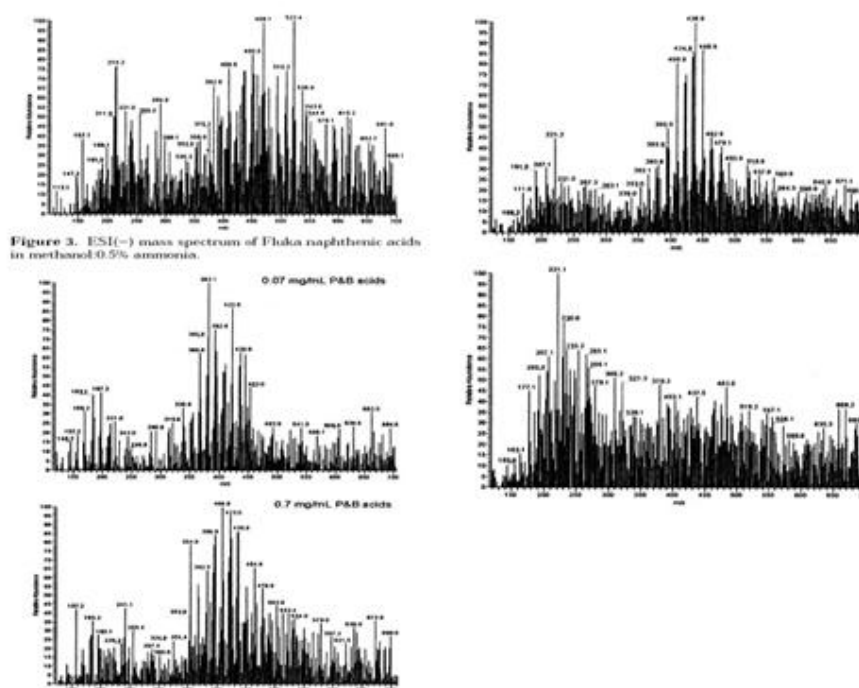


Figure 3. ESI(-) mass spectrum of Fluka naphthenic acids in methanol/0.5% ammonia.

Figure 1.4 – ESI (-) mass spectra of some acids

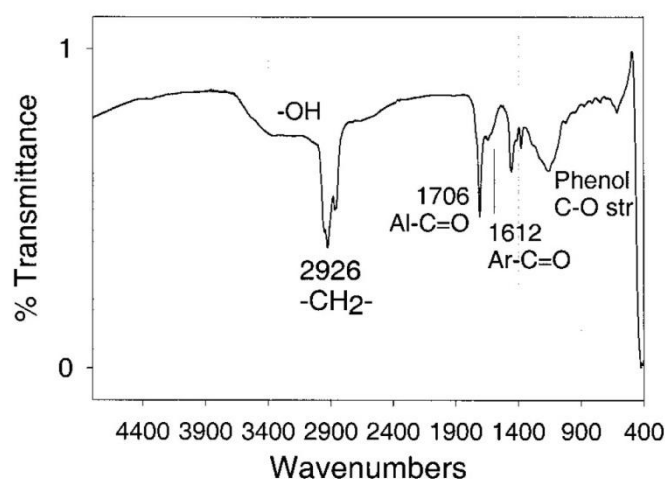


Figure 1.5 – Example of FTIR spectrum of an acid mixture extracted from a crude

FTIR spectroscopy allows identifying functional groups, and single, double and triple bonds. It is possible to identify acid carbonylic groups and to determine how they are bonded to the molecule (see Figure 1.5)<sup>5,9</sup>.

NMR Spectroscopy gives information about functional groups. By combining analyses with  $^1\text{H}$  and  $^{13}\text{C}$ , the technique has been useful in determining the average molecular structure of oil fractions<sup>44</sup>. In particular NAs that are in crude

---

oils show a peak that can be attributed to carboxylic hydrogen besides other peaks that can be attributed to hydrogens in aliphatic and aromatic hydrocarbons. Analyses with  $^{13}\text{C}$  indicate if the carboxylic group is bonded to aliphatic or aromatic carbons<sup>45</sup>.

Spectrometric analytical techniques allow the partial characterization of NA mixtures, concerning their molecular weight and composition. Even so a single technique is not able of determining the composition and the properties of a NA mixture.

#### 1.4. Testing equipment

Different kinds of tests are described in the literature to determine NA aggressiveness. Generally speaking three types of test may be found:

- Iron powder test;
- Confined environment tests;
- Hot oil flow loop test.

The *iron powder test*<sup>21,36,46,47,48</sup> was at first used to explore the corrosion kinetics of different cuts. It allows large excess of high specific surface iron powder (0.1 m<sup>2</sup>/g, 99.9%) to react with hot oil at different temperatures. Then dissolved iron is measured by means of ICP emission spectroscopy.

This test is fast and simple but doesn't provide a good repeatability and results depend on the employed iron powder. Moreover it doesn't take into account flow issues that are known to affect corrosion phenomena.

Concerning *confined environment*, tests may be conducted in glass flasks<sup>23,49,50,51,52</sup>, stainless steel vessels<sup>16</sup> or autoclaves<sup>18,35</sup> and with rotating<sup>24,53</sup> or static coupons. Test duration can be up to several days but in this case the testing fluid is continuously replenished. The configuration allows to verify the aggressiveness both in the liquid or vapour phase.

Tests have been carried out with crude<sup>18,19,35,50,53</sup>, single cuts<sup>19,50</sup>, or transformer oil<sup>16</sup>.

In the case of rotating coupons<sup>24,53</sup> it is possible to control mass transfer by regulating rotating speed (see Figure 1.6).



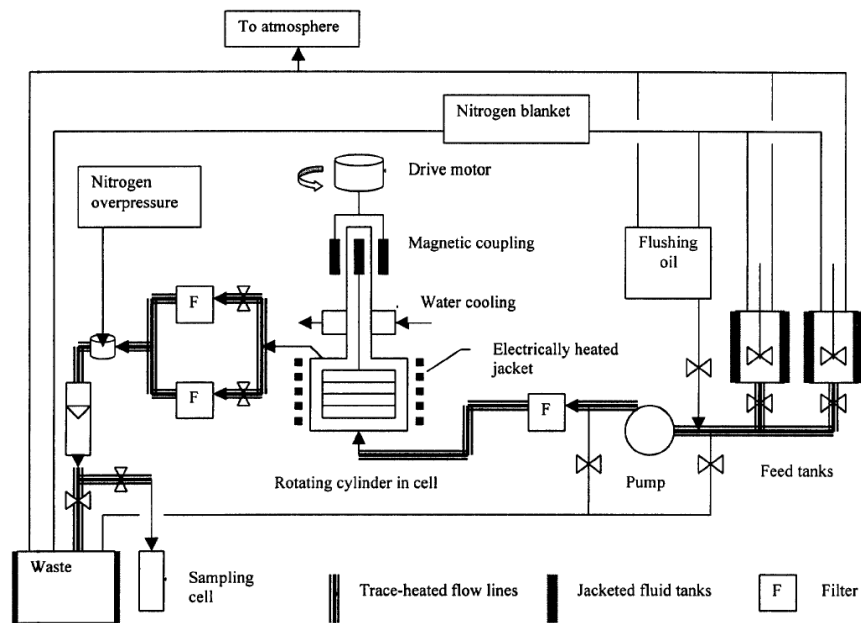


Figure 1.6 – Example of a plant for tests with rotating cylinder<sup>24</sup>

During the tests usually changes in the composition of the environment occur, due to gas evolution ( $\text{CO}_2$ ,  $\text{H}_2\text{S}$ ) or consumption of aggressive species. Hence it is preferable that for long test duration the testing fluid were replenished.

*Hot Oil Flow Loop and Jet-impingement*<sup>35,37,54</sup> employ a nozzle that generates particular flow dynamics conditions producing a very high flow rate on the surface of the coupons that is similar to operating conditions in furnace tubes or transfer lines. Impinging fluid may reach a speed of 49 m/s.



## 2. Experimental

### 2.1. Analytical characterization

Analyses were carried out by eni R&M SDM CHIF laboratories using three techniques: HPLC-ESI-MS, NMR and FTIR.

Mass spectrometry was used to qualitatively analyse acidic mixtures after extraction from crudes, then NMR and FTIR have been added both for quantitative and qualitative purposes. Moreover these last techniques can be used on crudes and their fractions without previous extraction.

#### 2.1.1. Mass Spectrometry

ElectroSpray Ionization (ESI) has been employed in negative ion configuration which is the most appropriate to detect acidic species. Separation by liquid chromatography was also considered as well as sample pre-treatment for acid extraction previous to analysis.

HPLC-MS analysis was done with Agilent HPLC1100 system with UV and ionic trap MS detectors. Ionisation was produced by an ESI source at 350 °C, 30 psi and 10 L/min inert gas. UV chromatograms were obtained at the following wavelengths: 260, 290 and 350 nm.

Chromatographic separation was conducted with Agilent Zorbax Eclipse XDB C8 (4.6 x 150 mm) column, with particles with 5 µm diameter. As mobile phase an acetonitrile and methanol (1:1) solution with 1% acetic acid was employed.

---

It was not possible to employ HPLC-ESI-MS directly on crude fractions, because signals of acids superimposed on matrix peaks.

A liquid-liquid extraction procedure was then implemented that comprises mixing of a solution of water and ethanol (50:50 vol.) with the sample at pH=11 by addition of drops of concentrated NH<sub>4</sub>OH. A two phase system was formed and then the aqueous phase was analysed without further treatment. Basification of solution showed to enhance chromatographic resolution and MS selectivity towards NAs.

### 2.1.2. NMR analysis

NMR analysis was conducted with a Varian spectrometer operating at 500.13 MHz (<sup>1</sup>H) and 125.76 MHz (<sup>13</sup>C) resonance frequencies. Samples were dissolved in deuterated chloroform and then analysed at proper impulse sequences. NMR does not need acids to be extracted prior to analysis. Table 2.1 shows the spectral intervals that were taken into account.

Table 2.1 – Spectral ranges of <sup>1</sup>H and <sup>13</sup>C NMR signals of NAs and main observed functionalities

<sup>1</sup> H		<sup>13</sup> C	
moiety	ppm	moiety	ppm
COOH	12	COOH	165-190
H arom	6.5-8	C arom	115-150
CH, CH <sub>2</sub>	4-1	CH, CH <sub>2</sub>	60-20
CH <sub>3</sub>	1-0	CH <sub>3</sub>	20-0

### 2.1.3. FTIR

FT-IR spectroscopy was conducted in air and at room temperature employing a Perkin-Elmer mod. 2000 spectrometer, in the wavelength range of 4000 – 400 cm<sup>-1</sup>, with 1 cm<sup>-1</sup> resolution. The liquid sample as received was placed in a cell with a path length of 0.5 mm and KBr crystal windows. This technique is used to determine the Naphthenic Acid Number (NAN) according to a proprietary procedure.

## 2.2. Materials

Corrosion tests were carried out on carbon (API X65, ASTM A210 A1, denoted below as CS) and low alloyed (ASTM A335 P5, denoted below as 5Cr) steels, in order to evaluate different behaviours with respect to the aggressive environment. Steels compositions are reported in Table 2.2.

Table 2.2 – Compositions of the steels employed for the experimental activity

Alloy	C	Mn	P	S	Si	Cr	Mo	Ni	Cu	V	Co	Fe
API X65	0.048	1.40	0.022	0.002	0.21	0.018	0.20	-	0.01	-	-	Bal.
ASTM A210 A1	0.13	0.7	0.011	0.007	0.22	0.04	0.015	0.08	0.2	0.005	0.03	Bal.
ASTM A335 P5	0.1	0.4	0.005	<0.001	0.32	4.8	0.5	0.12	0.15	0.007	0.02	Bal.

## 2.3. Testing environment

Tests were conducted in different environments: preliminary tests (in autoclave see Chap. 3) in crude oil, then a new testing configuration was used with gasoil and a commercial mixture of NAs added to it. Subsequently real crudes were also employed.

### 2.3.1. Gasoil

Gasoil was chosen because it is the typical cut where NAs concentrate in crude distillation units. A *blue diesel without detergents* was used as hydrocarburic matrix without spurious interactions with the corrosive phenomenon.

The employed gasoil was provided by eni R&M Division and its properties are reported in Table 2.3, whereas the cut points are displayed in Table 2.4.

Table 2.3 – Main properties of the gasoil used for tests

Parameter	Value
H <sub>2</sub> O content	25 ppm
Density @15° C	0.842 g/ml
Flash point	53 °C
TAN	0.2 mg <sub>KOH</sub> /g

---

Table 2.4 – Gasoil cut points

<b>Initial Boiling Point /°C</b>	<b>% Off</b>
170	1.2
280	46.8
330	74.4
350	81.0
400	88.2
500	93.1
>750	97.4

### 2.3.2. Naphthenic acid mixture

A NA commercial mixture by Umicore N.V., namely DNA 200-215 SR, was used to introduce acids in the environment. Figure 2.1 shows the ESI spectrum obtained and Table 2.5 reports NMR data. It is possible to observe that the mixture consists mainly of molecules with one and two rings (i.e. Z=-2 and -4) centred between twelve and nineteen carbon atoms, whereas there are only few compounds with higher Z.

Figure 2.2 shows NMR spectra of the mixture: a large band is present between 10 and 50 ppm, because of the complexity of cyclic structures which produces superimposed spectral lines.

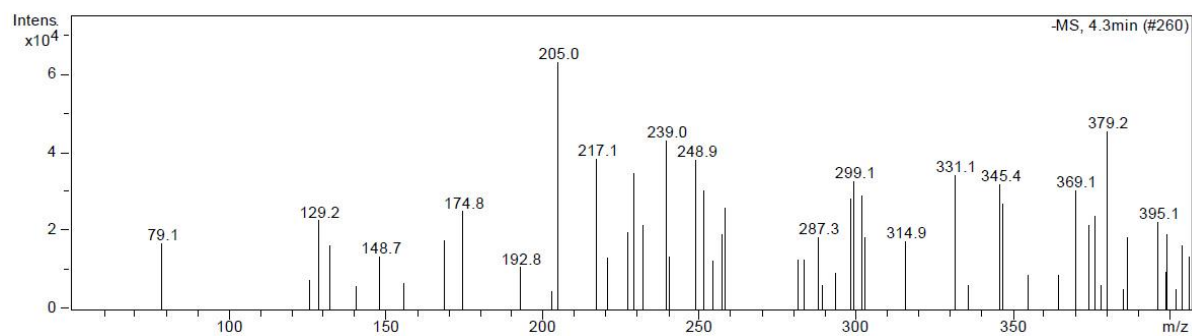


Figure 2.1 – ESI (-) spectrum of the NA commercial mixture used in the tests

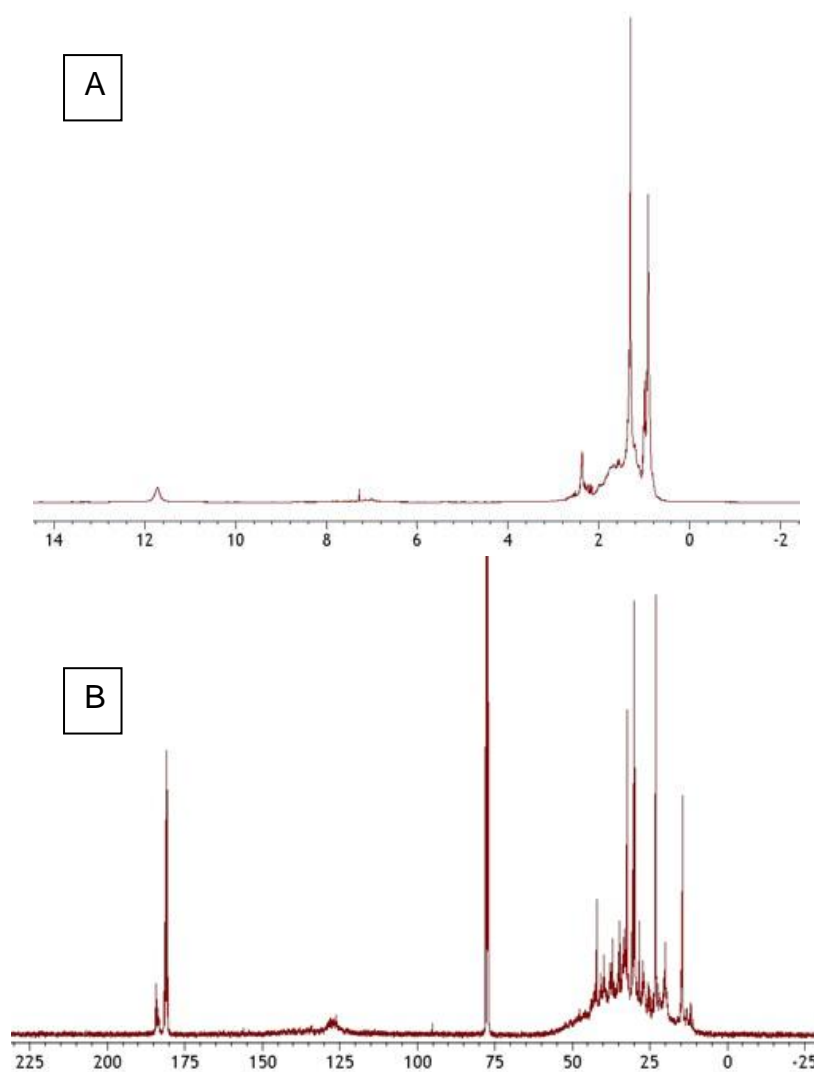


Figure 2.2 – NMR spectra of the NA commercial mixture. (A)  $^1\text{H}$ ; (B)  $^{13}\text{C}$

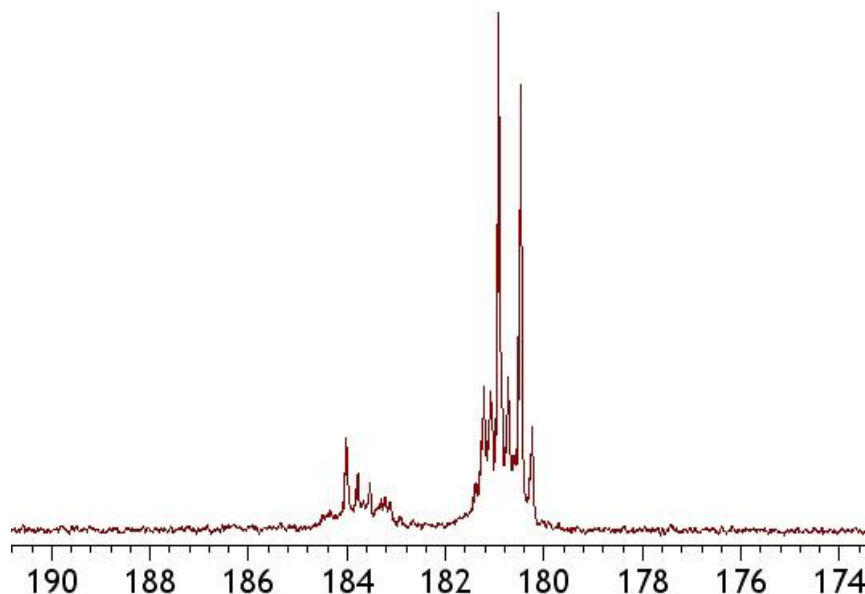


Figure 2.3 –  $^{13}\text{C}$  spectrum of the carboxylic groups: mainly primary acids are evident

Table 2.5 – Molar % distributions of H and C in NAs

<b>H</b>	<b>(%mol)</b>
COOH	3.2
Har	1.8
CH,CH <sub>2</sub>	68.9
CH <sub>3</sub>	26.1
<b>C</b>	<b>(%mol)</b>
COOH	6.1
Car	6.5
Cal	87.4

Carboxylic group distribution is shown in Figure 2.3: the range 172 – 175 ppm refers to groups bonded to aromatic carbons, 178 – 182 ppm to groups bonded to primary  $-\text{CH}_2$  and 182 – 188 ppm to groups bonded to secondary  $-\text{CH}$ . It is possible to observe that signals of aromatic carboxylic groups are not present and  $-\text{COOH}$  groups are mainly bonded to alkyl chains. Percent distributions are reported in Table 2.6.



Table 2.6 – Molar % distribution of primary and secondary acids

-CH <sub>2</sub> -COOH	77%
>CHCOOH	23%

If we assume that each NA has only one carboxylic group, the following molecular formula and average Z can be calculated:

C<sub>15.4</sub>H<sub>30.2</sub>COOH (MW=260 g/mol; Z=-1.6)

From the average molecular weight it is possible to calculate the corresponding TAN value, using the following formula:

$$\text{TAN mg}_{\text{KOH}}/\text{g} = n(\text{mol/g}) * \text{MW}_{\text{KOH}}(\text{g/mol}) * 1000$$

And the result is:

$$\text{TAN} = 1/260 * 56 * 1000 = 215 \text{ mg}_{\text{KOH}}/\text{g}.$$

### 2.3.3. Crude samples

Crude samples were provided by eni R&M Division. Crude reference and main characteristics are reported in Table 2.7.

Table 2.7 – Main characteristics of the crude used in corrosion tests

Crude	API gravity @ 60° C	Density @ 15° C	Sulphur %	TAN /mg <sub>KOH</sub> /g
<b>A</b>	16.6	0.9546	2.57	1.58
<b>B</b>	11.2	0.9912	3.82	2.87
<b>C</b>	28.3	0.8851	2.73	0.34
<b>D</b>	29.0	0.8811	2.13	0.18
<b>E</b>	45.3	0.7998	0.12	0.06
<b>F</b>	27.5	0.8896	0.36	0.85

## 2.4. Corrosion tests equipment

All tests were carried out at Venezia Tecnologie SpA laboratories in Venice.

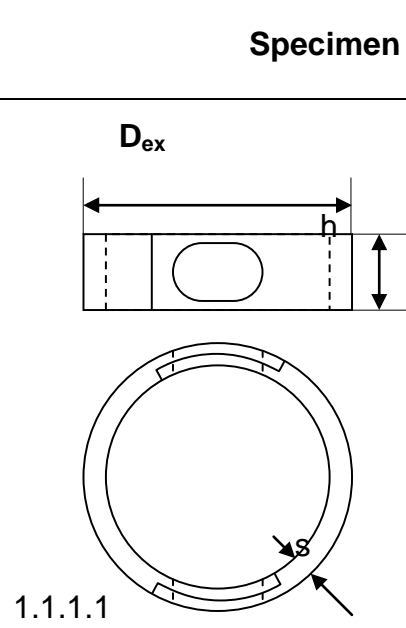
#### 2.4.1. Autoclave configuration

First exploratory tests were carried out using already existing equipment, i.e. autoclaves.

Test parameters and specimens geometry were selected on the basis of a previous work.

Specimens were in the shape of half a ring, so that it was possible to examine two coupons per test. The assembled ring rotated around a diameter (see Table 2.8 and Figure 2.4 and 2.5).

Table 2.8 – Specimen geometry for HT-HP tests

Specimen dimensions		
	External diameter	60 mm
	Thickness	5 mm
	Height	17 mm

A one litre Hastelloy C276 autoclave was employed, allowing a maximum temperature of 350° C and a maximum pressure of 350 bar.

Crudes acidity was determined before and after tests by potentiometric titration according to ASTM D664. Initial and after test sulphur content in the oil was determined by XRF technique.

Tests were performed using the parameters described in Table 2.9.

#### *Testing Procedure*

Oil and specimens are loaded into the autoclave and then the system is kept in nitrogen flow for 15 minutes; then the heating begins. Each test is assumed to start when the target temperature is reached. At the end the system is cooled down and degassed.

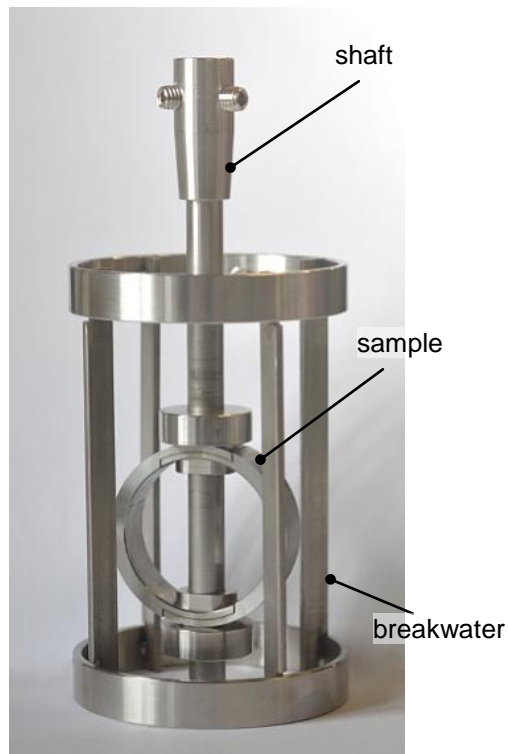


Figure 2.4 – HT-HP testing configuration



Figure 2.5 – HT-HP specimen mounted in the autoclave

---

Table 2.9 – HT-HP test matrix

<b>Temperature</b>	270°C – 350°C
<b>Rotation speed</b>	600 rpm
<b>Material</b>	API 5L X65 – 5Cr 1Mo
<b>Duration</b>	24 – 72 hours

#### 2.4.2. Small plant for crude corrosiveness assessment

Tests in autoclave highlighted the limits of this kind of experiments. In fact, gas evolution was observed (pressure increase during the test), in particular the oil decomposition produced high quantities of H<sub>2</sub>S that caused specimen sulphidation.

Although an attempt was made to separate sulphidation and NA attack contribution to corrosion of coupons, it was decided to design a completely new facility that could be capable of simulating plant operating condition avoiding oil degradation by gas evolution and thermal cracking.

The main features of a new equipment to assess a crude corrosiveness should have been:

- a multi-step heating section;
- a short residence time in the hot section to avoid degradation of the testing fluid;
- high fluid velocity on the surface of coupons (no rotating cage-like testing section).

These features were obtained with the small plant described in Figure 2.6.

The plant comprises a feeding jacketed vessel, from where the testing fluid is pumped through the system, a two step heating area which consists of a counter-current exchanger and an electrical heating section, then there is the testing section and afterwards the fluid cools down in the exchanger and goes back to the vessel. There are several pressure and temperature sensors in order to control experimental conditions and for the safety of the operating personnel.

At the beginning of the test the vessel can be heated by a heating tape (in case of heavy oils) whereas during the experiment it is possible to provide further cooling in the jacket.

The plant was built according to European Pressure Equipment and ATEX Directives and was also CE marked.

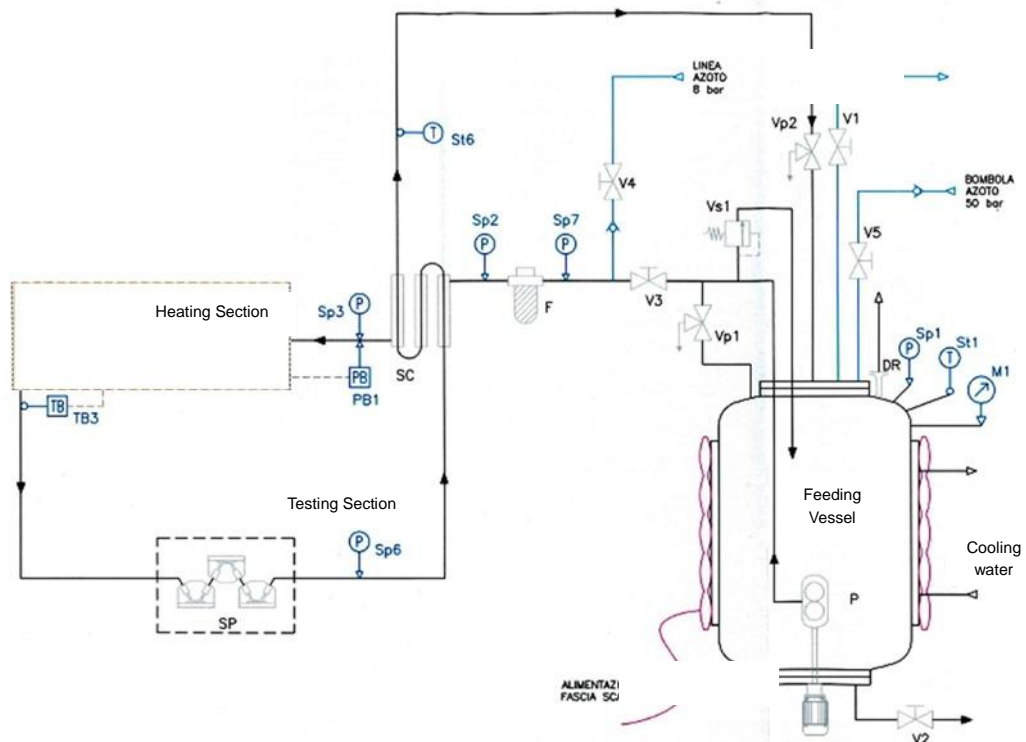
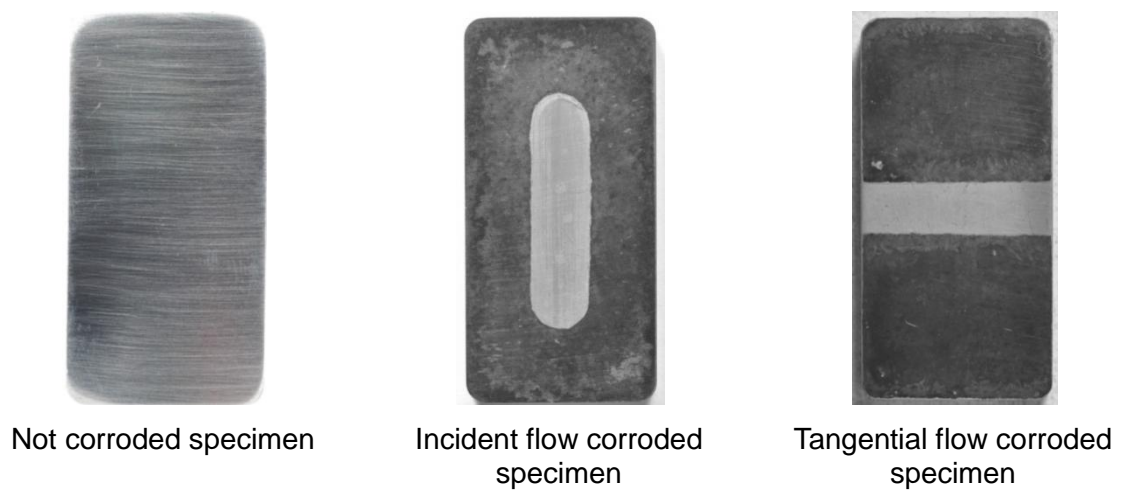


Figure 2.6 – Small plant to determine crude corrosivity



Not corroded specimen

Incident flow corroded specimen

Tangential flow corroded specimen

Figure 2.7 – Specimen geometry and appearance

---

Specimens are shaped as plates (Figure 2.7), which are 40 mm wide, 20 mm high and 30 mm thick.

Before tests they are polished with emery paper up to P600 grit. Then they are degreased in acetone and weighed prior to each test. After the test they are rinsed with toluene and acetone and then corrosion products are removed by pickling the exposed area. The specimens are then weighed again and the total weight loss can then be determined.

Two kinds of coupon holder were designed in order to study different situation: the incident- and the tangential-flow coupon holder (Figure 2.8). The first was designed to determine what happens in the curves of furnace tubes and transfer-lines, whereas the second may be used to study other conditions (linear parts, column, etc.).

The variation of the system pressure (pressure in the feeding vessel) can control the amount of evaporation and as a consequence the velocity in the hot section of the plant.

#### *Testing procedure*

First the specimens are placed in the holder, then the fluid is preheated in the vessel whereas nitrogen flows in all the plant tubes. Subsequently the feeding vessel is pressurised, the fluid is pumped in the system, and the electrical heating starts. At the end of the test the heating is stopped and the oil is cooled down. At low temperature the tubes are drained by nitrogen flow. Afterwards specimens are retrieved.

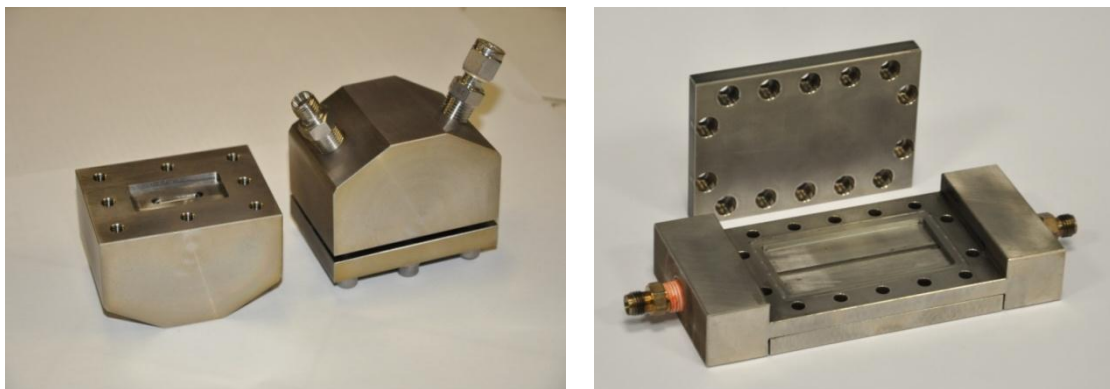


Figure 2.8 – Incident flow specimen holder (left); tangential flow specimen holder (right)

### 2.5. Corrosion rate evaluation

Corrosion rate was calculated by the weight loss method according to ASTM G1 standard by using the following formula:

\_\_\_\_\_

where CR is corrosion rate in mm/y  
 $\Delta w$  is mass loss in g  
 $A$  is surface area in  $\text{cm}^2$   
 $t$  is time of exposure in hours  
 $\rho$  is material density in  $\text{g/cm}^3$ .

### 2.6. Experimental design

#### 2.6.1. Introduction<sup>55</sup>

Many experimental situations require the examination of the effects of varying two or more factors. In a complete exploration of such a situation it is not sufficient to vary one factor at a time, but all combinations of the different factor levels must be examined in order to determine the effect of each factor and the possible ways in which each factor may be modified by the variation of the others. In the analysis of the experimental results the effect of each factor can be estimated with the same accuracy as if only one factor had been varied at a time, and the interaction effects between the factors can also be evaluated. Following some definitions are reported.

The term *factor* is used to denote any feature of the experimental conditions which may be assigned from one trial to another.

The various values of a factor examined in an experiment are known as *levels*.

The set of levels of all factors in a given trial is called the *treatment*.

The numerical result of a trial based on a given treatment is called the *response* corresponding to that treatment.

The *effect* of a factor is the change in response produced by a change in the level of the factor. There are *main effects*, i.e. the average effect of one factor over all the levels of the other factors and *interactions*, i.e. when the effect of one factor is different at different levels of another factor.

---

### 2.6.2. 3<sup>2</sup> full factorial experimental plans<sup>55</sup>

A 3<sup>2</sup> experimental plan describes a series of treatments varying two factors over three levels for a total number of nine treatments. Indicating with -1 the lower level, 1 the higher one and 0 the intermediate one, it is possible to construct the following table for treatments.

Table 2.10 – 3<sup>2</sup> Full factorial plan

Treatment	Factor A	Factor B
1	-1	-1
2	-1	0
3	-1	1
4	0	-1
5	0	0
6	0	1
7	1	-1
8	1	0
9	1	-1

Generally treatments should be carried out in random order to obtain independent observations, excluding unsuspected causes of disturbance

When all the responses are determined, the Analysis of Variance is carried out in order to determine which of the effects and interactions are statistically significant. The non significant ones may then be discarded and a response surface may be constructed which represents the model fitting the experimental data.

### 2.6.3. Employed factors, levels and treatments

A 3<sup>2</sup> full factorial experimental plan was prepared to examine how NAs and sulphur may interact and to separate their contribution to corrosion. Levels for TAN value and sulphur content are reported in Table 2.11.

Table 2.11 – Factors and levels for the experimental plan

Parameter	Low	Medium	High
TAN	0.5	0.7	1
S%	0.5	1	2.1



These values were selected considering ranges that were acceptable for real processes in refineries with a metallurgy consisting mainly of carbon steel.

Tests were conducted at 350°C with a liquid phase velocity of 0.5 m/s, corresponding to a velocity in the multiphase section of 20 m/s (transfer line simulation), and lasted three days. Two specimens for each material underwent the same test and were considered as replica of the same condition.

The plan was not randomised because of the small quantities of available crude oils. As a consequence, first the mixture with the proper sulphur content was prepared and then the right quantity of NAs was added from time to time to the same oil mixture in order to obtain the desired TAN value. Thus each mixture was used to carry out three treatments.

The statistical analysis of the experimental plan was carried out by using Statistica 9.0 software by StatSoft. All analyses were carried out considering a 95% of confidence interval and a value of significance level  $\alpha$  of 0.05.



## 3. HT – HP testing

Preliminary tests were conducted in autoclave with the aim of determining the general corrosiveness of some crude oils.

Two materials were used for the tests: API 5L X65 micro-alloyed steel and 5Cr 1Mo steel.

After each test, corrosion rate was estimated from weight loss and specimens were examined with optical microscopy for localized damage.

Three oils were used, namely A, B and C, where C is a blend of 50% B and 50% of a synthetic oil.

Crudes acidity was determined before and after tests by potentiometric titration according to ASTM D664. Initial and after test sulphur in the oil was determined by XRF technique.

### 3.1. Results and discussion

Test conditions and results are summarized in Table 3.1.

Since the phenomenon of high temperature corrosion in crude oil is very complex, results of tests need a through discussion.

Two mechanisms of corrosion are active:

- Acid corrosion, mainly due to NA content. As already stated, the parameter mainly used to range crude oil corrosiveness is TAN number, whose validity

is under scrutiny. In fact, a high TAN can be due to different acids (not only naphthenic) present in the crude and naphthenic acids aggressiveness is not directly related to acidity.

- Sulphide corrosion: Sulphur is a corrosion inhibitor at low concentration; concentration higher than ~0.2% can increase corrosion rate because the sulphide layer which is formed is no more protective. Corrosion rate in this case is also strongly dependent on flow rate.

Table 3.1 – HT- HP tests results and crudes analyses

Oil	Temp. (°C)	P <sub>max</sub> (bar)	Rotating rate (rpm)	Test duration (days)	Average corrosion rate (mm/y)	Material	S content %		TAN	
							Initial	After test	Initial	After test
A	270	8	600	3	0.10	API 5L X65	2.57	2.4	1.58	1.55
	350	50	600	3	2.74	API 5L X65		2.1		0.95
	350	24	600	3	2.10	API 5L X65		1.9		0.82
	350	30	600	1	2.63	API 5L X65	2.57	2.2	1.58	1.1
	350	14	600	1	2.26	5Cr		2.1		0.36
	350	18	600	3	1.57	5Cr		1.7		0.3
B	350	28	600	1	3.85	5Cr	3.64	2.6	2.87	0.68
	350	22	600	3	2.97	5Cr		2.5		<0.5
C	350	21	600	1	1.52	5Cr	2.73	2.4	0.34	<0.2
	350	24	600	3	1.09	5Cr		2.2		<0.2

Before commenting corrosion rate results it is worthwhile highlighting how the environment changes during the test. In fact total sulphur content and TAN values decrease because of the degradation of the testing fluid due to the permanence at high temperature for so a long period of time.

The effect of sulphur is mainly due to the presence of H<sub>2</sub>S evolving from the crude, the concentration of which is not simply related to sulphur content. In fact, during the tests the pressure increases (figure 3.1), because of cracking of hydrocarbons, sulphur compounds (evolving H<sub>2</sub>S) and organic acids and by light hydrocarbons evaporation. The main problem of autoclave tests is that the environment is confined, so that the evolved H<sub>2</sub>S concentrates in the fluid.

Hydrogen sulphide is responsible for the high corrosion rate experienced by carbon steel in the second test with A oil (test duration: 3 days; corrosion rate: 2.74 mm/y;  $T=350^{\circ}\text{C}$ ). So the subsequent tests were conducted at a lower pressure (maximum 25 bar) by periodically degassing the autoclave. A condenser was used to avoid light hydrocarbon loss. This had the purpose of limiting  $\text{H}_2\text{S}$  partial pressure in the gas phase and highlighting naphthenic acid corrosion.

Comparison between corrosion rates of 5Cr and carbon steel in A oil, shows that chromium steel has a moderate higher corrosion resistance.

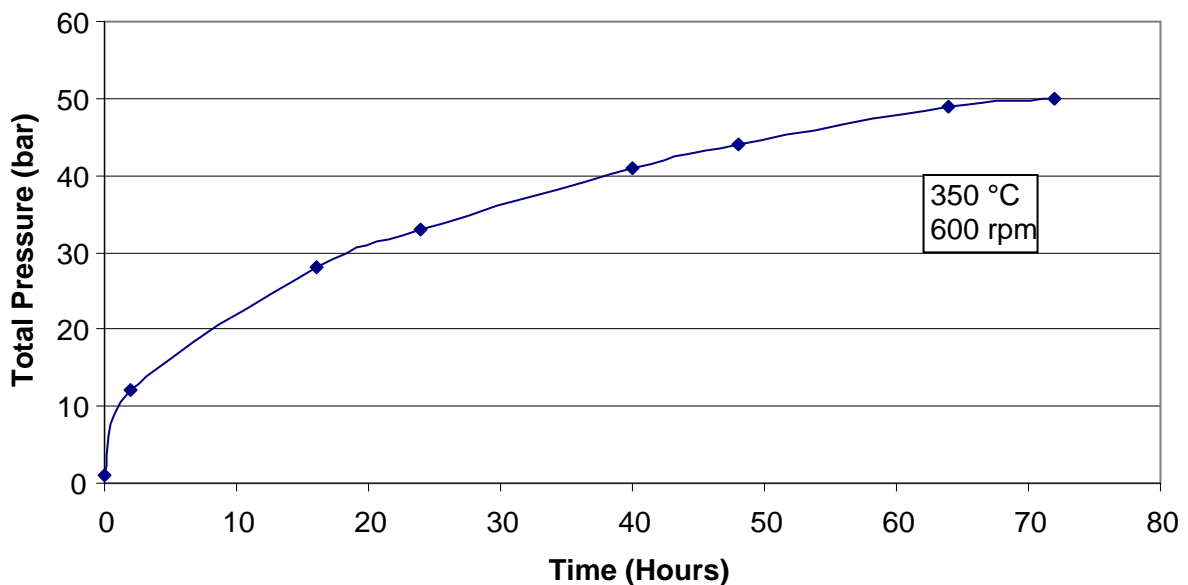


Figure 3.1 – Pressure increase during a three days test with A oil

In figure 3.2, corrosion rate in different crude oils is plotted vs. sulphur content and TAN with the aim of highlighting the influence of each single parameter on corrosion rate.

Comparing the results of 5Cr steel it can be observed that corrosion rate increases with TAN value, but it must be underlined that A is a B blend, so the two points are interdependent.

The comparison of analytical data about sulphur content and TAN may represent the respective contributions on corrosion rate.

Considering data of A and B oils related to one day tests, it is possible to observe that TAN value decreases significantly (from 1.58 to 0.36 and from 2.87 to 0.68,

respectively). In the same test time, sulphur content decreases slightly (from 2.57% to 2.1% and from 3.64% to 2.6%, respectively). Therefore it is reasonable to suppose that NA corrosion is negligible after the first day of test. Assuming that NAs contribute to corrosion only during the first day and that H<sub>2</sub>S contributes during all test days, the respective corrosion rates can be calculated as reported in Table 3.2.

The reliability of NA corrosion rate data reported in Table 3.2 can be addressed when comparing the corrosion rates of A and C.

Both A and B crudes cause NA attack and high temperature sulphidation but the latter is the predominant phenomenon in the autoclave test configuration.

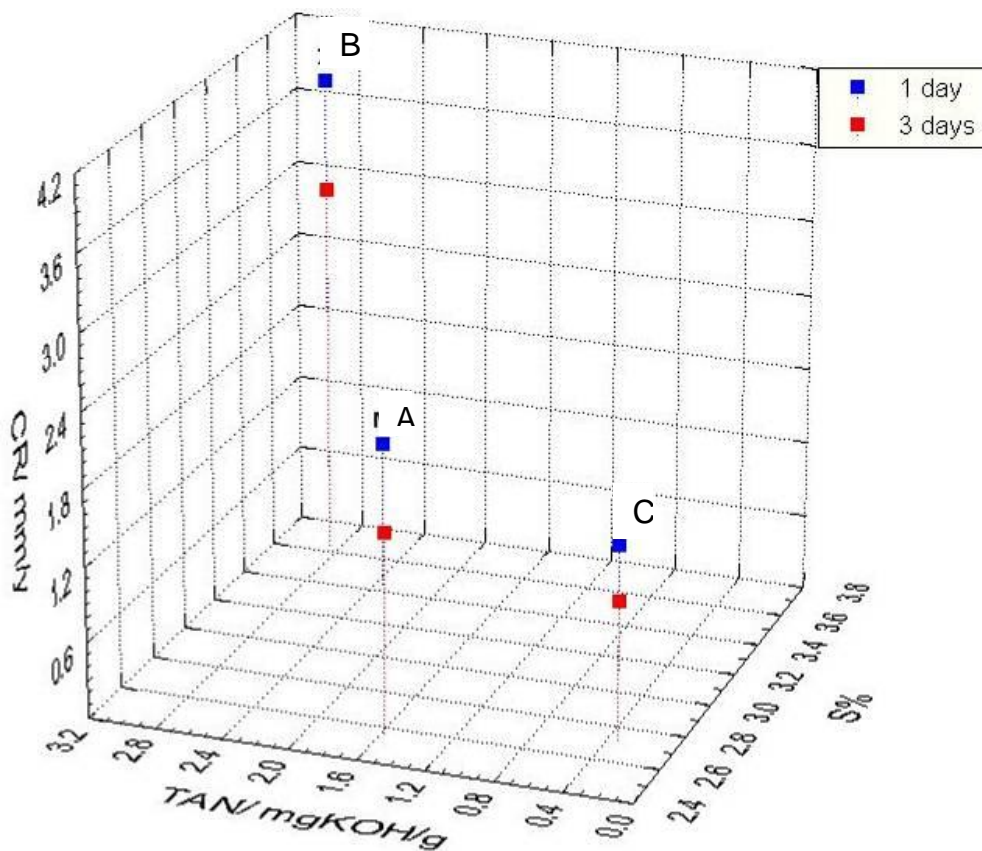


Figure 3.2 – Corrosion rate of A, B and Coils vs. TAN and S content

Table 3.2 – Calculated H<sub>2</sub>S and NAs contributions to corrosion rate (A data are reported for comparison)

Oil	Total corrosion rate (mm/y)	H <sub>2</sub> S corrosion rate (mm/y)	NA corrosion rate (mm/y)
A	1.57	1.25	0.32
B	2.97	2.48	0.49
C	1.09	1.09	n/a

### 3.1.1. Stereomicroscope examination

After tests, specimens were removed from the autoclave, cleaned and examined with stereomicroscope. Figures 3.3 to 3.7 report the pictures taken at 50X magnification: surface appearance confirms that the main phenomenon is high temperature sulphidation.

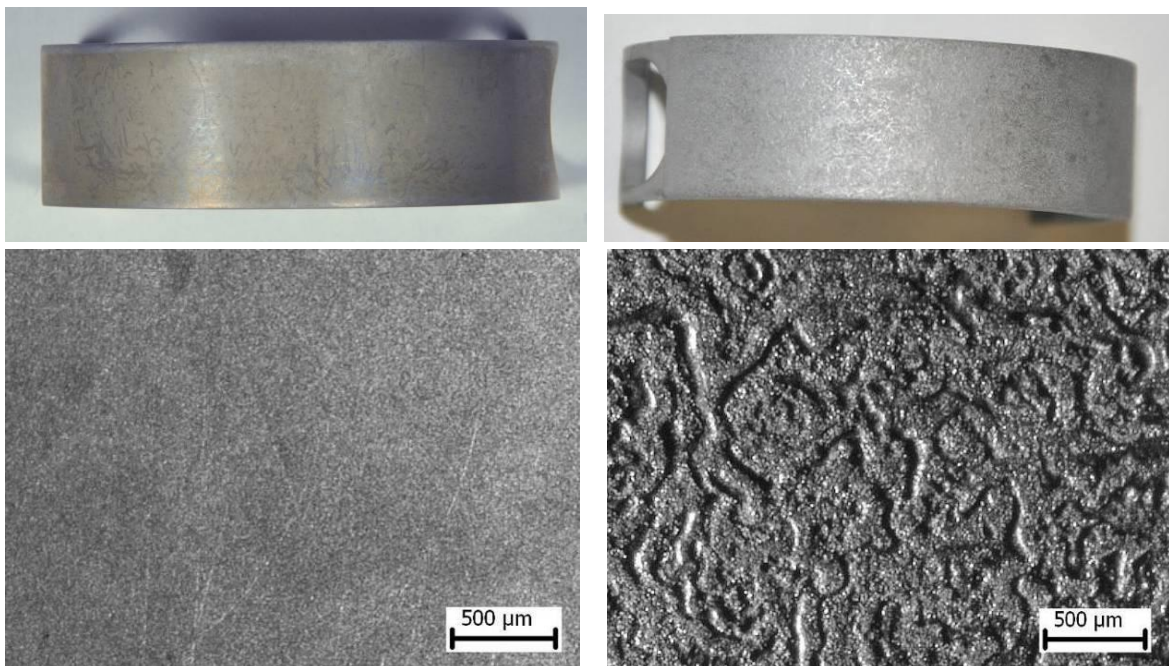


Figure 3.3 – API 5L X65 carbon steel specimens after 3 days tests in A oil, without degassing, at 270°C (on the left) and 350°C (on the right)

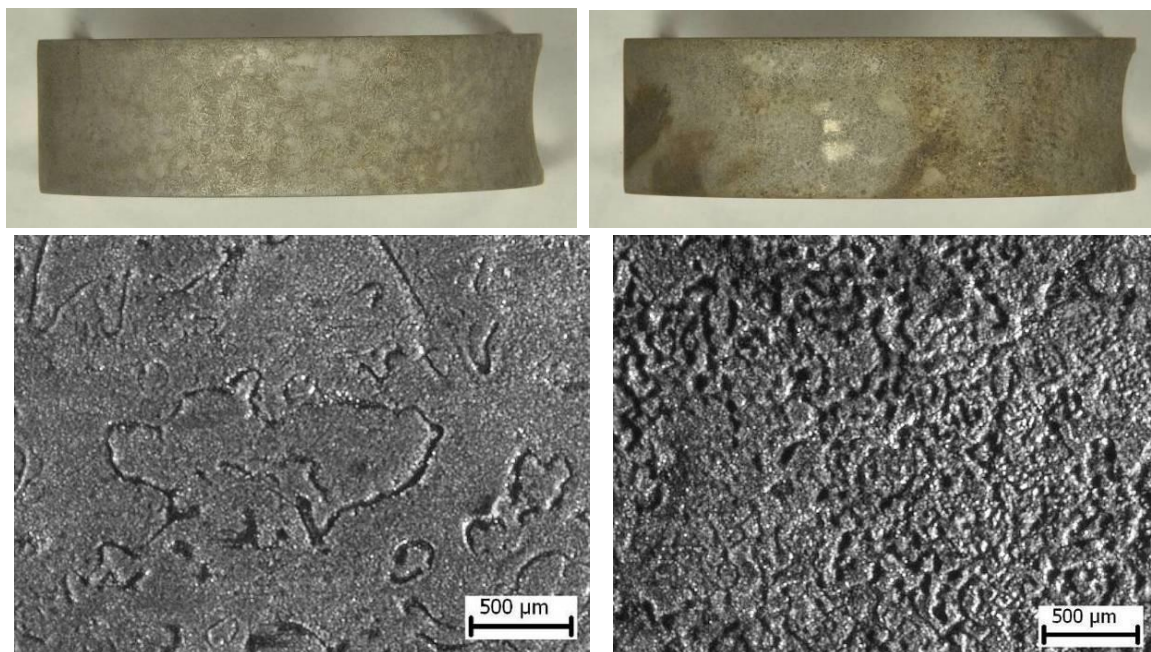


Figure 3.4 – API 5L X65 specimens after 1 day (on the left) and 3 days (on the right) tests in A oil, at 350°C, with autoclave degassing

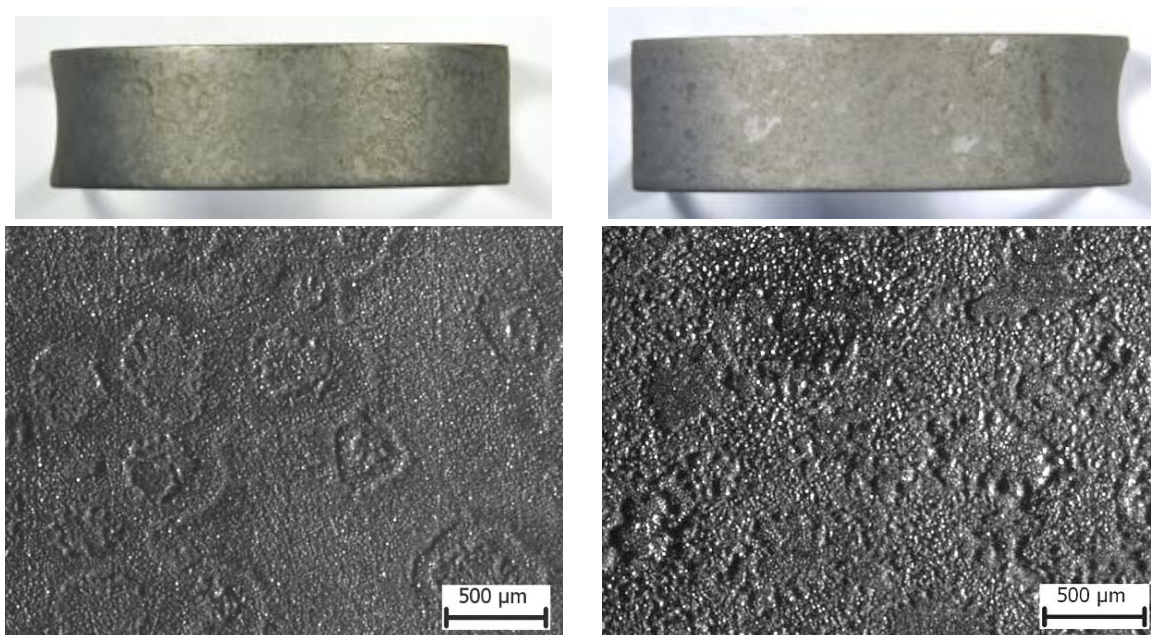


Figure 3.5 – 5Cr specimens after 1 day (on the left) and 3 days (on the right) tests in A oil, at 350°C, with autoclave degassing



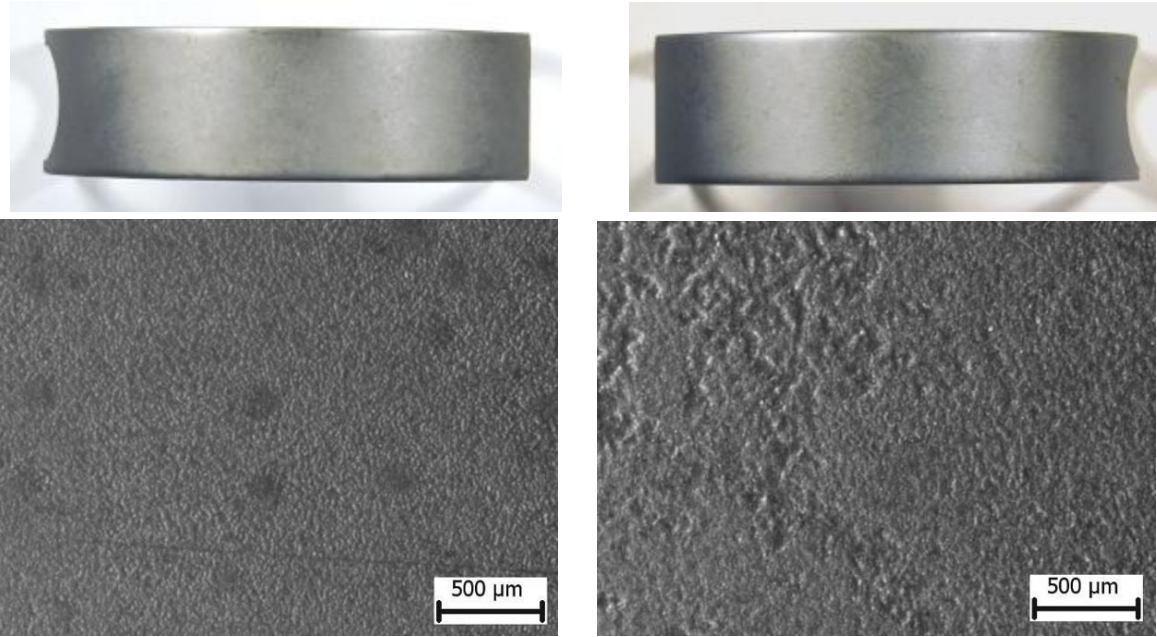


Figure 3.6 – 5Cr specimens after 1 day (on the left) and 3 days (on the right) tests in C oil, at 350°C, with autoclave degassing

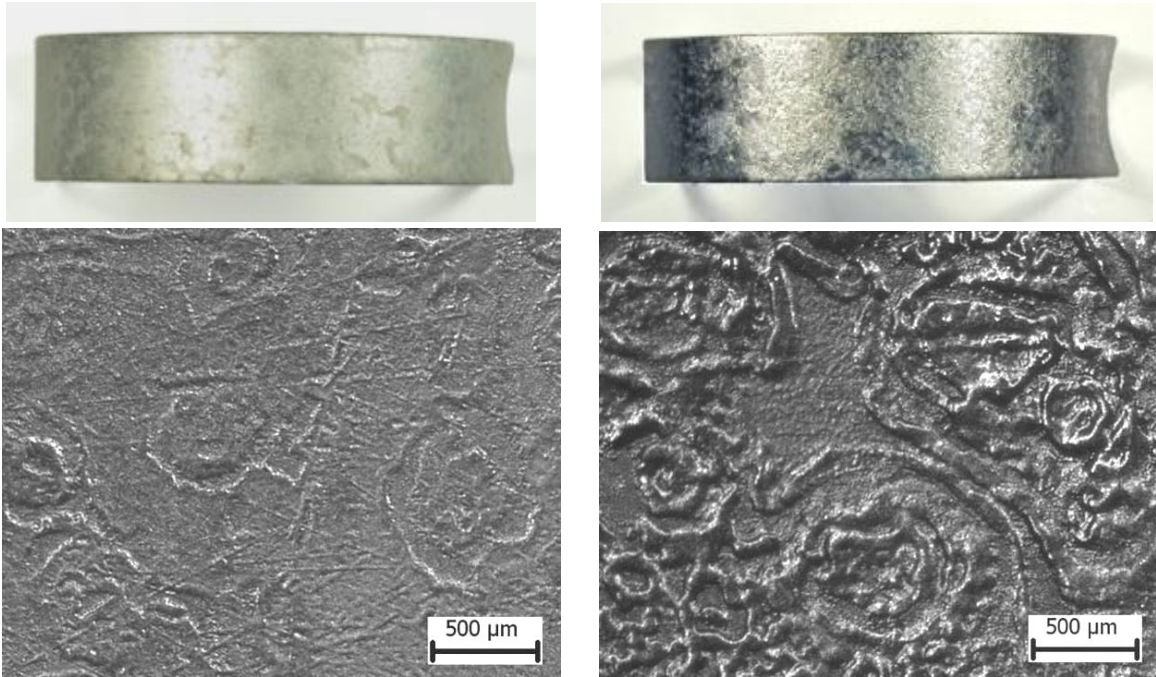


Figure 3.7 – 5Cr specimens after 1 day (on the left) and 3 days (on the right) tests in B oil, at 350°C, with autoclave degassing

---

### **3.2. Remarks**

Autoclave tests results provided information about some differences in the aggressiveness of the oil employed. Anyway results give only a general indication and it is difficult to correlate them with crude units corrosion phenomena. Moreover the environment continuously changes because of fluid degradation occurring at the employed temperature.

Therefore a different kind of test is needed that allows to control the environment composition in a better way and to simulate real operating conditions. Furthermore it is essential not to cause fluid degradation in order to keep constant the concentrations of aggressive and inhibitive species for the whole test duration.

## 4. Small plant for crude corrosivity

### 4.1. Plant validation

Some tests were conducted to evaluate if the plant were able to discriminate between fluids with different aggressiveness and with the aim of determining corrosion detection limit.

As testing fluid a mixture of gasoil without additives and a NA mixture by Umicore was used.

Corrosion tests were carried out in different conditions to determine how temperature, fluid velocity, NA concentration and test duration may affect corrosion rate.

Table 4.1 reports test conditions and results; corrosion rates are averaged over two coupons.

Table 4.1 – Tests with gasoil and NA commercial mixture

Test	TAN	Duration /d	Temperature /°C	Pressure /bar	Material	Flow and velocity of the liquid phase /m/s	Corrosion rate /mm/y
7 (reference)	0.2	3	330	7	5Cr	Incident / 0.4	<0.05
3	2.2	1		7	5Cr	Incident / 0.4	<0.05
4		3			5Cr	Incident / 0.4	0.17
5		5			5Cr	Incident / 0.4	0.14
6		3			5Cr	Incident / 0.4	0.23
2	4.2	1		7	5Cr	Incident / 0.4	1.07
1	6.1	1		7	5Cr	Incident / 0.4	3.0
8	4.2	1	280	7	5Cr	Incident / 0.4	0.10
9					A210	Incident / 0.4	0.15
10	4.2	1	330	7	5Cr	Tangential/ 0.4	0.69
					A210		0.89
11					5Cr	Tangential/ 0.9	1.14
					A210		1.34
12					5Cr	Tangential/ 3	1.94
					A210		2.15

It is possible to observe that:

- Corrosion rate increases with the acidity of the fluid (see Figure 4.1) and tests longer than one day are needed to measure low corrosion rates (TAN 2.2 mg<sub>KOH</sub>/g).
- A pressure decrease produces higher evaporation that causes an increase in fluid velocity and this generates a higher corrosion rate as it happens by increasing the flow rate (see Figure 4.2).
- Corrosion rate increases with temperature.
- Carbon steel and 5Cr steel behave in the same manner towards NA attack.
- There is no significant effect due to tangential or incident coupon holder.
- Corrosion product layers are not produced on coupon surfaces and corrosion rate doesn't change with test duration.

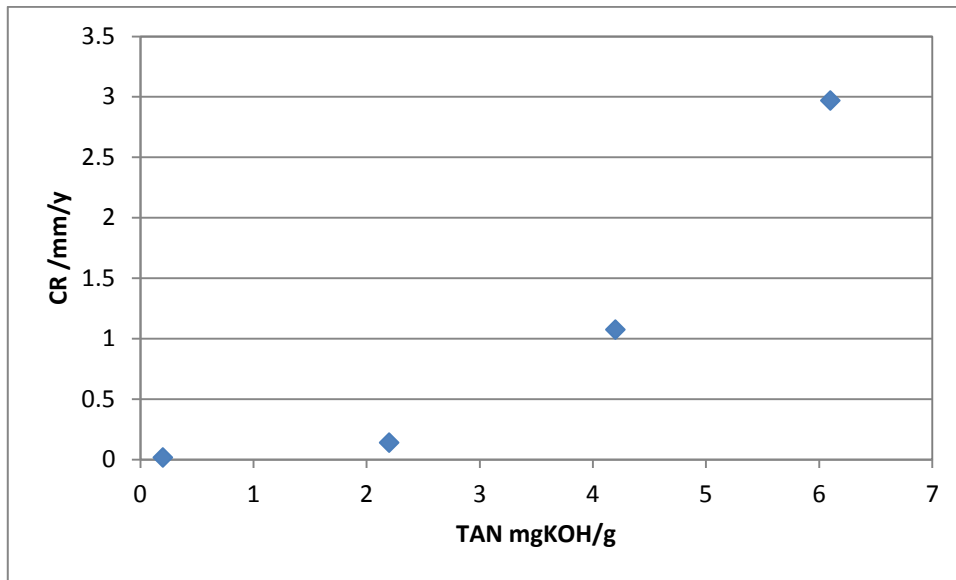


Figure 4.1 – Corrosion rate vs. TAN; test conducted on 5Cr for 24 hours at 330°C; incident flow, 0.4 m/s

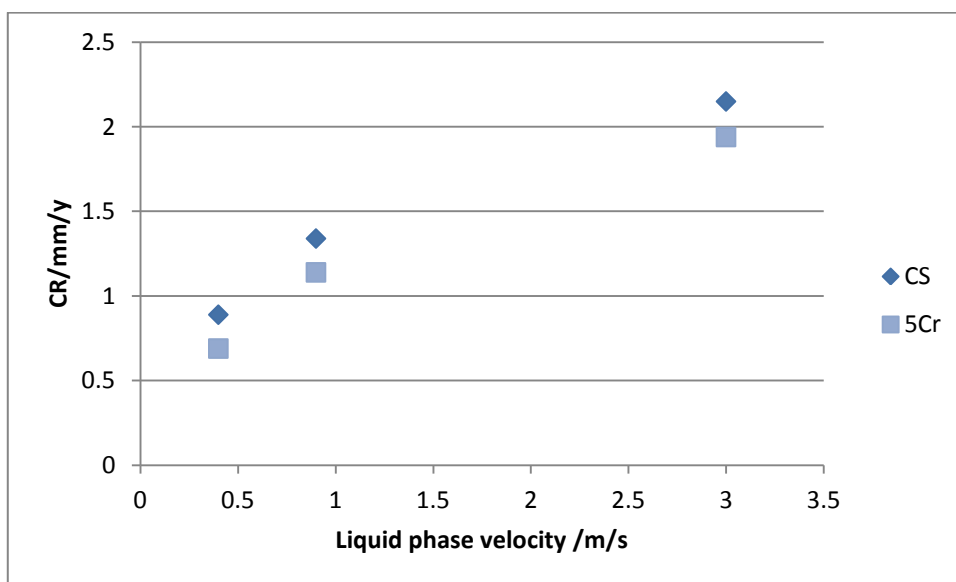


Figure 4.2 – Corrosion rate vs. flow velocity; test conducted at TAN 4, 330°C, for 24 hours; tangential flow

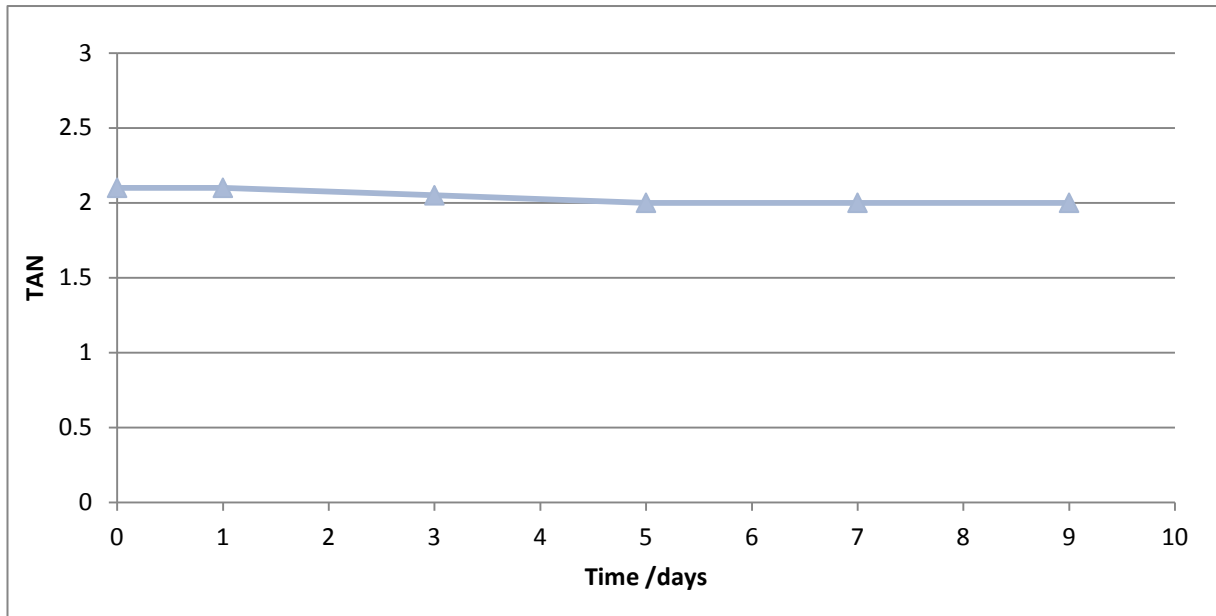


Figure 4.3 – TAN trend with test duration at 350°C

Concerning fluid degradation, ESI-MS analysis was conducted before and after the test besides TAN value measurement whose value doesn't change (see Figure 4.3).

Figure 4.4 shows ESI-MS spectra of DNA in gasoil at TAN 2, as received, and after three and eight days of corrosion test at 330° C: it is possible to observe that even if NA concentration doesn't change because of the test, there seems to be a variation in molecular structure. In fact, the formation of structures with two naphthenic rings is promoted with respect to acyclic structures or with only one ring. Moreover there is a decrease of the quantity of molecules with 16 and 18 carbon atoms, with the formation of lighter molecules with 15, 14 and 11 carbon atoms. This may be due to molecular cracking or rearrangement caused by temperature or interaction with the metal.

On the basis of the previous considerations it is possible to say that the plant achieves the targets, which it was designed for.

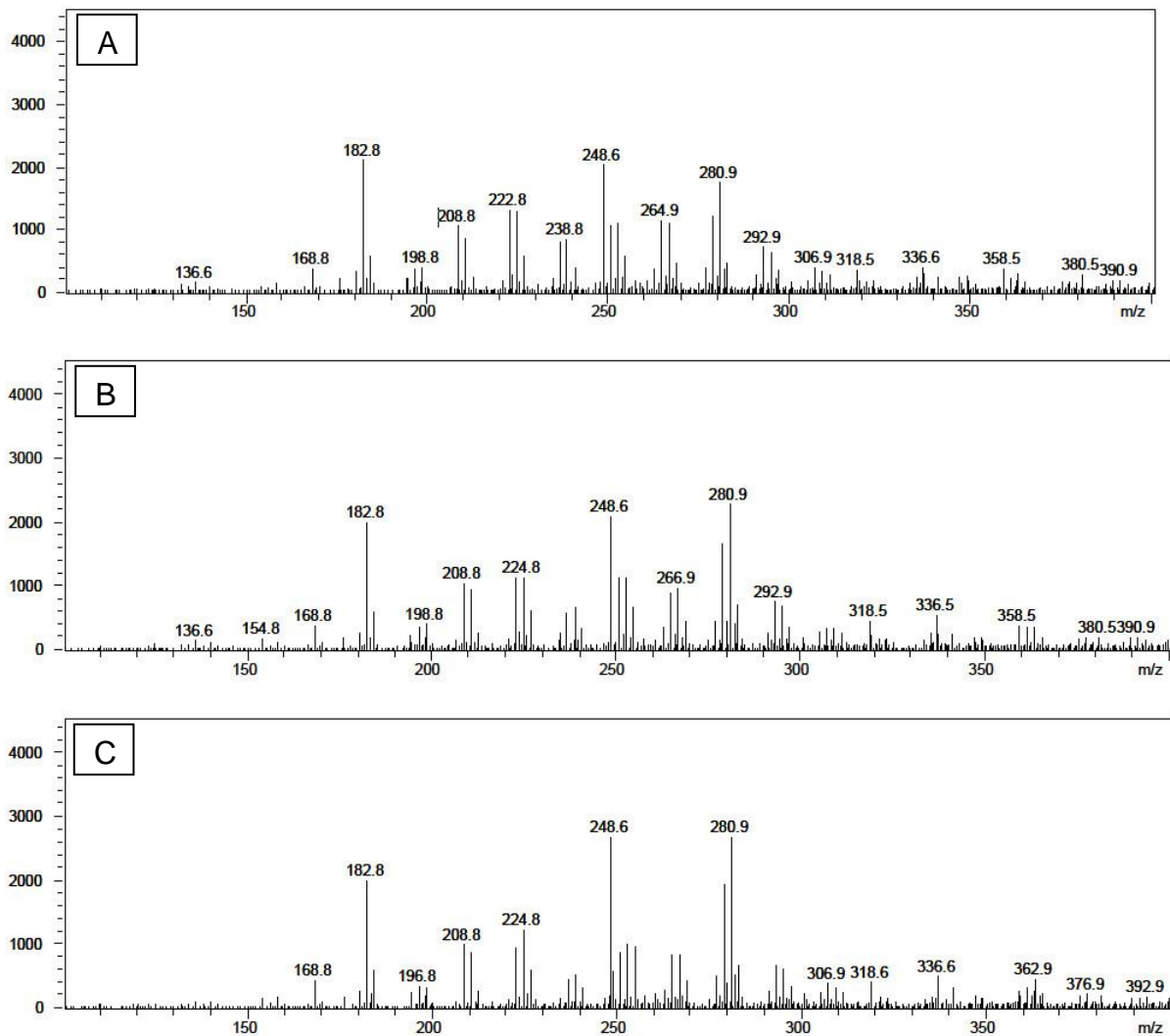


Figure 4.4 – ESI(-)-MS spectra of the extracted acids from a mixture gasoil-NA at initial TAN 2: (a) initial; (B) after 3 days of test; (C) after 8 days of test

## 4.2. Tests with crudes

After first tests with gasoil and NA commercial mixture, experiments were carried out with real crudes. On the basis of their availability a low sulphur content (Sahara Blend, S 0.12%) and a high sulphur content (Iranian Heavy, S 2.1%) were chosen with the aim of setting two “blank” references for the following experiments.

### 4.2.1. Low sulphur crude

The low sulphur crude allows to avoid interaction with NA corrosion phenomenon due to sulphur compounds.

Test matrix and results are reported in Table 4.2.

Table 4.2 – Test matrix and results for tests with low sulphur crude

TAN	Vessel pressure /bar	Liquid phase velocity /m/s	CS CR /mm/y
0.06	4	0.4	<0.05
0.5	4	0.7	0.1
0.5	2	0.7	0.2

At the highest acid concentration two levels of pressure were applied: the pressure controls the amount of vapour phase, hence the velocity in the testing section of the plant. All tests lasted five days and were carried out at 350° C using the incident flow specimen holder. Only 5Cr steel was tested in these conditions.

It is possible to observe that even at so low NA concentrations corrosion rate is not negligible, moreover increasing flow velocity intensifies the aggressiveness of the environment.

#### 4.2.2. High sulphur crude

Tests were conducted at 350° C, without the addition of NAs. Test results are reported in Table 4.3.

Tests evidenced the different behaviour of the materials: 5Cr steel is in fact more resistant toward high temperature sulphidation. Modified McConomy curves are commonly used to predict corrosion rate depending on the temperature, metallurgy and sulphur content<sup>56</sup>. By comparing results with the corresponding values from the curves (Figure 4.5 and Table 4.4), we find that they are quite consistent for carbon steel and too high for 5Cr steel. This issue will be addressed in the discussion section.

Table 4.3 – Test results for high sulphur crude at 350° C

Duration /days	5Cr CR /mm/y	CS CR /mm/y
1	1.72	3.89
2	1.28	2.01
4	1.01	1.89



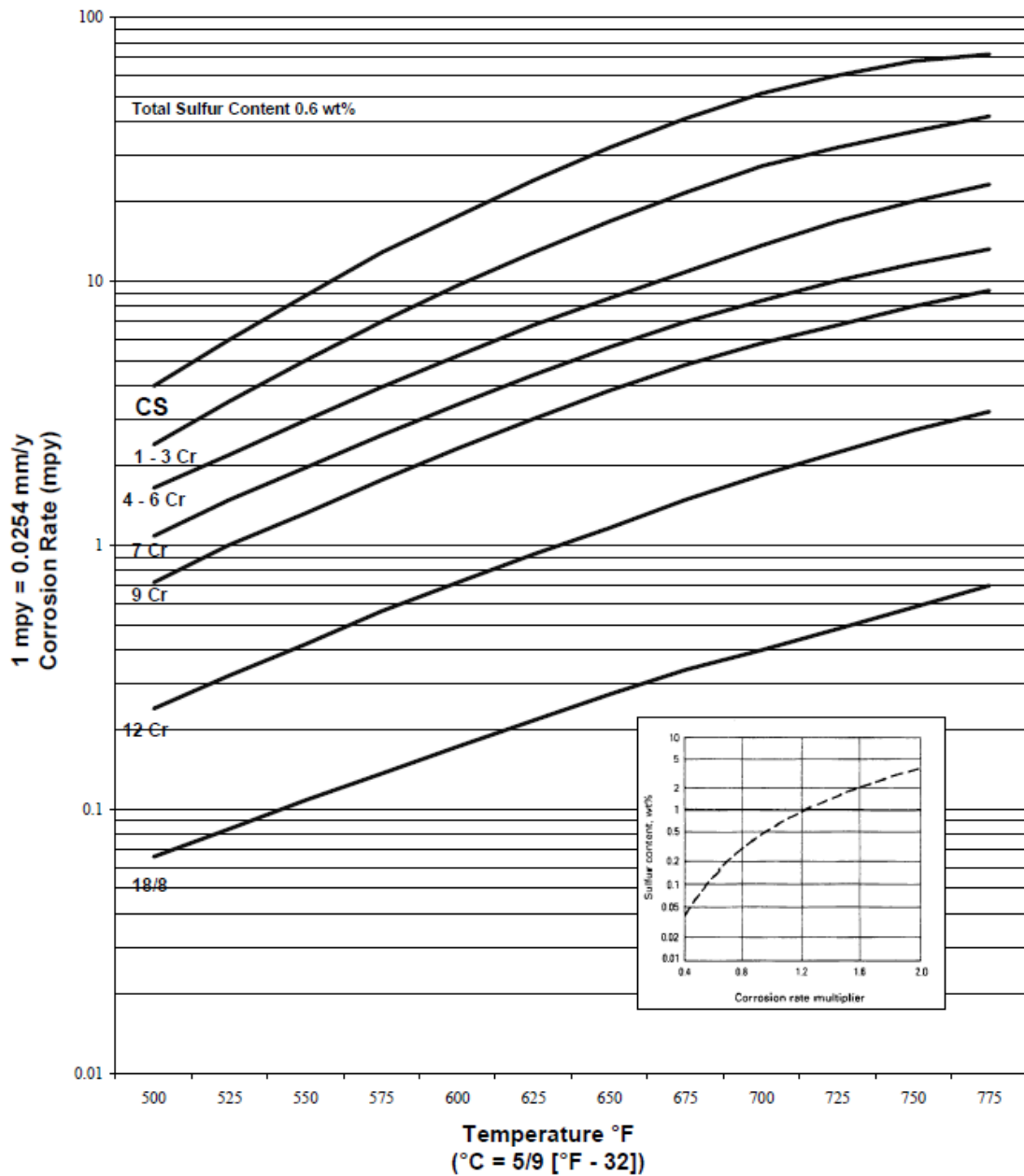


Figure 4.5 – Modified McConey curves

Table 4.4 – Comparison of experimental corrosion rates and values from modified McConey curves

Material	CR @ 0.6%S	Estimated CR	Experimental CR
CS	1.02	1.63	1.89
5Cr	0.30	0.48	1.01

---

### 4.3.3<sup>2</sup> factorial plan results and analysis

Details of the full plan together with measured corrosion rates are reported in Table 4.5.

Table 4.5 – Test matrix and results for the experimental plan

Case number	TAN	S%	CR CS /mm/y	CR 5Cr /mm/y
1	0.5	2.1	2.12	0.99
2	0.5	2.1	2.25	1.25
3	0.7	2.1	2.16	1.09
4	0.7	2.1	2.55	1.35
5	1.0	2.1	3.14	1.56
6	1.0	2.1	3.22	1.40
7	0.5	1.0	1.02	0.36
8	0.5	1.0	0.78	0.36
9	0.7	1.0	0.91	0.84
10	0.7	1.0	0.86	0.88
11	1.0	1.0	1.40	0.87
12	1.0	1.0	1.48	0.90
13	0.5	0.5	0.63	0.47
14	0.5	0.5	0.66	0.57
15	0.7	0.5	0.52	0.64
16	0.7	0.5	0.64	0.51
17	1.0	0.5	0.97	1.26
18	1.0	0.5	1.19	1.20

The first comment considering results is that all treatments caused high corrosion rates in both materials. However it is possible to observe that at high sulphur contents (entries n.1 to 6) 5Cr steel corrodes less than CS, whereas at low sulphur contents (entries n.13 to 18) the two materials almost behave in the same way.

As an example Figure 4.6 shows the appearance of one carbon steel specimen after the test: the central part of the channel where the fluid flow exhibit no continuous FeS layer, while the pickled surface shows the initiation of some localised corrosion.

Figure 4.7 shows the appearance of 5Cr steel surface: also in this case the corrosion product layer is discontinuous and the pickling revealed the presence of localised attack. These features were common to almost all treatments.

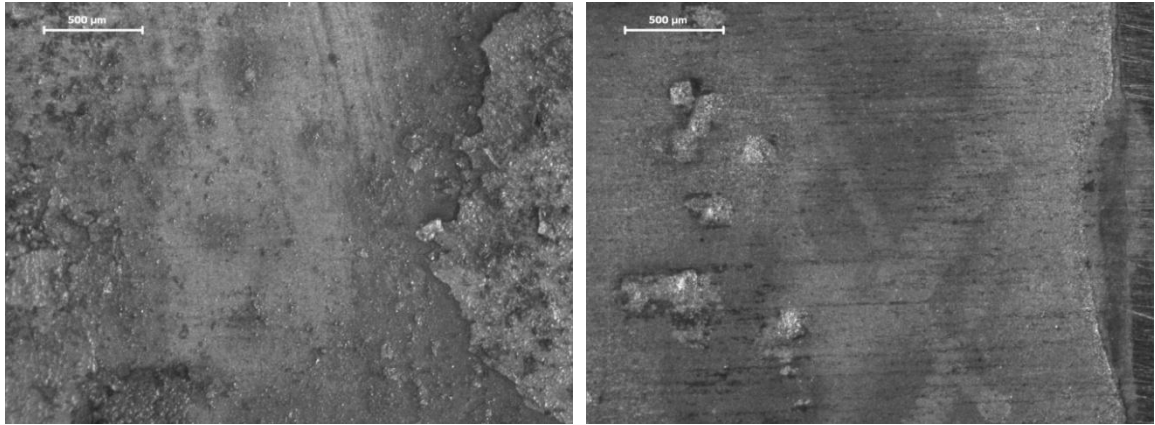


Figure 4.6 – Appearance of CS coupon after treatment n.13

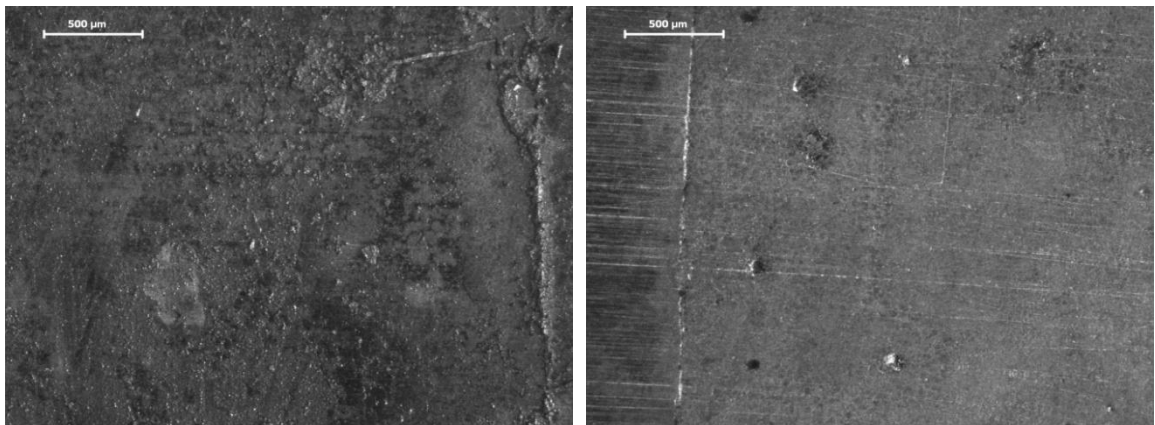


Figure 4.7 – Appearance of 5Cr steel after treatment n.13

Analyses of results are reported separately for CS and 5Cr steels.

#### 4.3.1. Carbon steel data analysis

Figure 4.8 shows different plots of corrosion rate data for CS: it is possible to say that the distribution is quite far from normality.

It is possible to try to transform data to obtain a better normal-like distribution. As a first approach for a right skewed set of data it is possible to apply natural logarithm. As it is possible to observe in Figure 4.9 the transformation is reasonable and the new data have good normality.

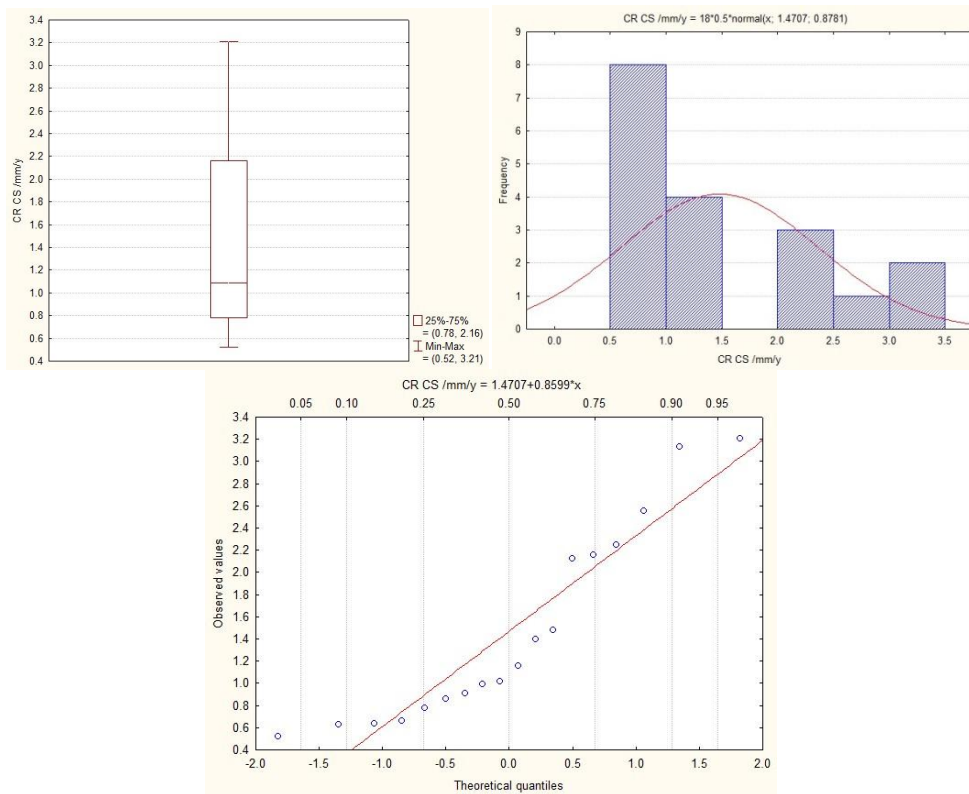


Figure 4.8 – Box-plot, histograms and normal probability plot for CS CR variable

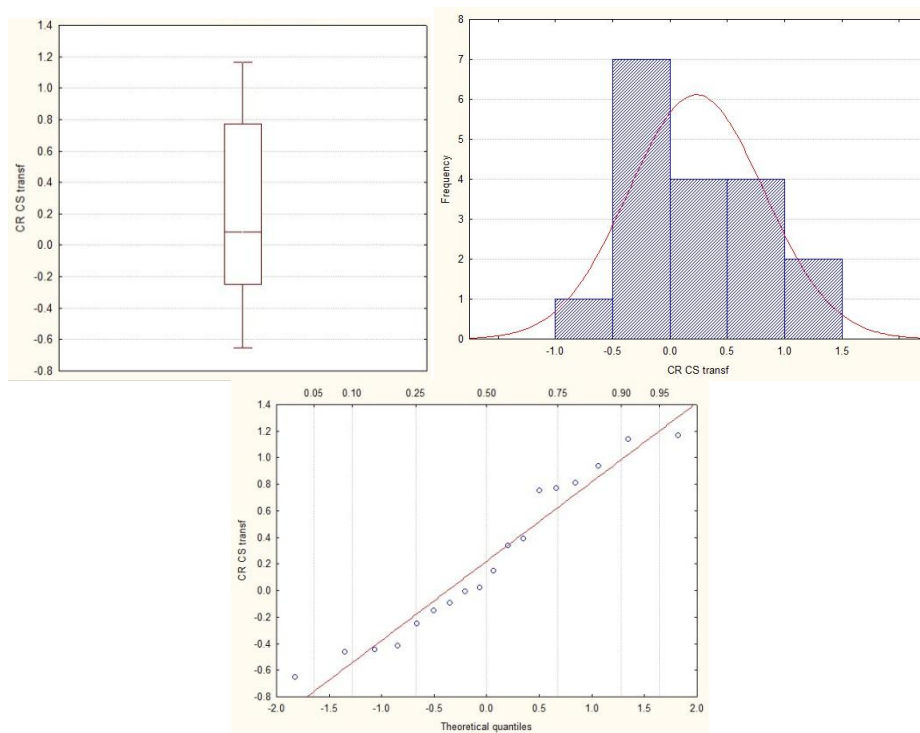


Figure 4.9 – Histograms, box-plot and normal probability plot for transformed variable  $\ln(\text{CS CR})$

It could be possible to apply Box Cox transformation for further improvement, but in this case, for modelling and predictive purposes, it is preferable to avoid too complex transformations.

### Theoretical model

For a  $3^2$  full factorial experiment it is possible to fit a model containing a mean term (intercept), two main effect linear terms, two main effect quadratic terms, then one second order interaction term, two third order interaction terms and one fourth order interaction term.

The theoretical model has then nine unknown constants. The ANOVA table for such a model is reported in Table 4.6.

Table 4.6 – ANOVA table of the complete model for  $\ln(\text{CS CR})$

	SS	DF	MS	F	p
<b>(1)TAN (L)</b>	0.578836	1	0.578836	57.7975	0.000033
<b>TAN (Q)</b>	0.128241	1	0.128241	12.8051	0.005945
<b>(2)S% (L)</b>	4.519541	1	4.519541	451.2824	0.000000
<b>S% (Q)</b>	0.005140	1	0.005140	0.5132	0.491918
<b>1L x 2L</b>	0.009235	1	0.009235	0.9221	0.361999
<b>1L x 2Q</b>	0.000109	1	0.000109	0.0109	0.919114
<b>1Q x 2L</b>	0.037015	1	0.037015	3.6960	0.086710
<b>1Q x 2Q</b>	0.001389	1	0.001389	0.1387	0.718171
<b>Error</b>	0.090134	9	0.010015		
<b>Total SS</b>	5.865372	17			

The related  $R^2$  is 0.985 and adjusted  $R^2$  is 0.971.

It is possible to observe that interactions except for 1Qx2L are not statistically significant, since the related p-values are quite high. Figure 4.10 shows the half normal probability plot of effects: it should be possible to simplify the model discarding some terms such as linear interaction term (1Lx2L), fourth order interaction (1Qx2Q) term and the non significant third order term (1Lx2Q). However It is preferable to keep sulphur quadratic term, since it is one main effect.

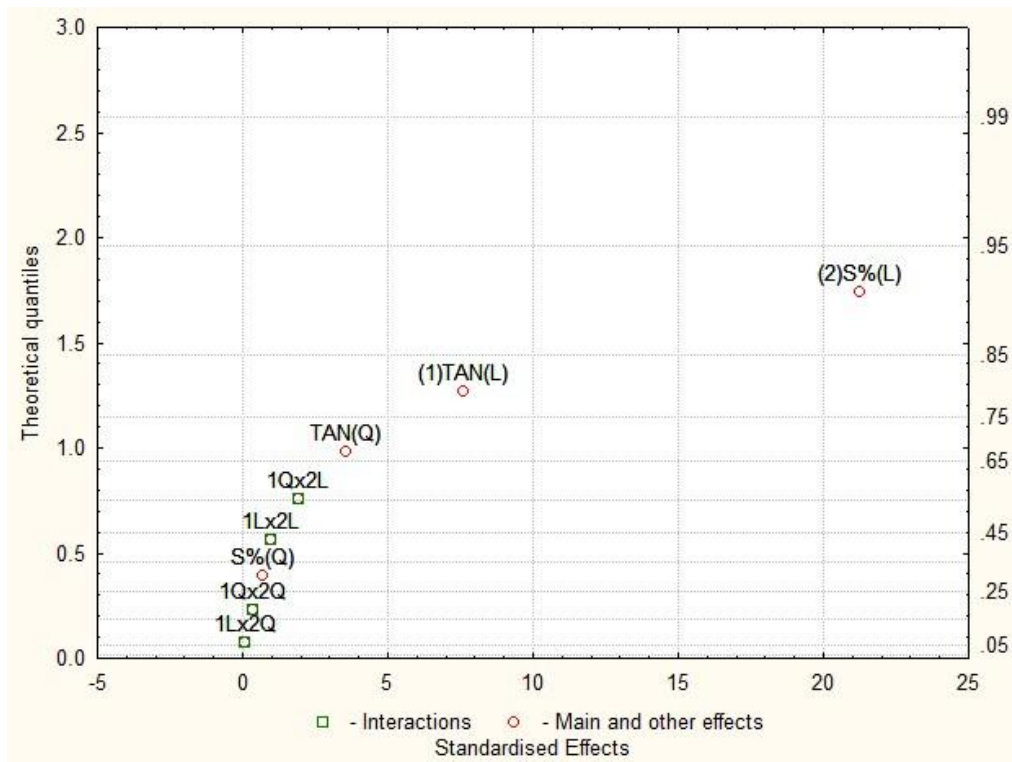


Figure 4.10 – Half-normal probability plot of the effects for ln(CS CR)

Table 4.7 reports the ANOVA results for the simplified model that has an  $R^2$  of 0.983 and an adjusted  $R^2$  of 0.976.

For completeness of the analysis it must be said that the addition of one more term would not improve the model much more, generating an adjusted  $R^2$  of 0.976.

Hence the final model comprises linear and quadratic terms for each factor and one third order interaction term.

Table 4.7 – ANOVA table for the simplified model

	SS	DF	MS	F	p
<b>(1)TAN (L)</b>	0.615266	1	0.615266	72.6119	0.000002
<b>TAN (Q)</b>	0.128042	1	0.128042	15.1112	0.002159
<b>(2)S% (L)</b>	4.583206	1	4.583206	540.8969	0.000000
<b>S% (Q)</b>	0.005298	1	0.005298	0.6252	0.444465
<b>1Q x 2L</b>	0.040662	1	0.040662	4.7989	0.048953
<b>Error</b>	0.101680	12	0.008473		
<b>Total SS</b>	5.865372	17			

## Residual analysis

Figure 4.11 reports different plots for residuals.

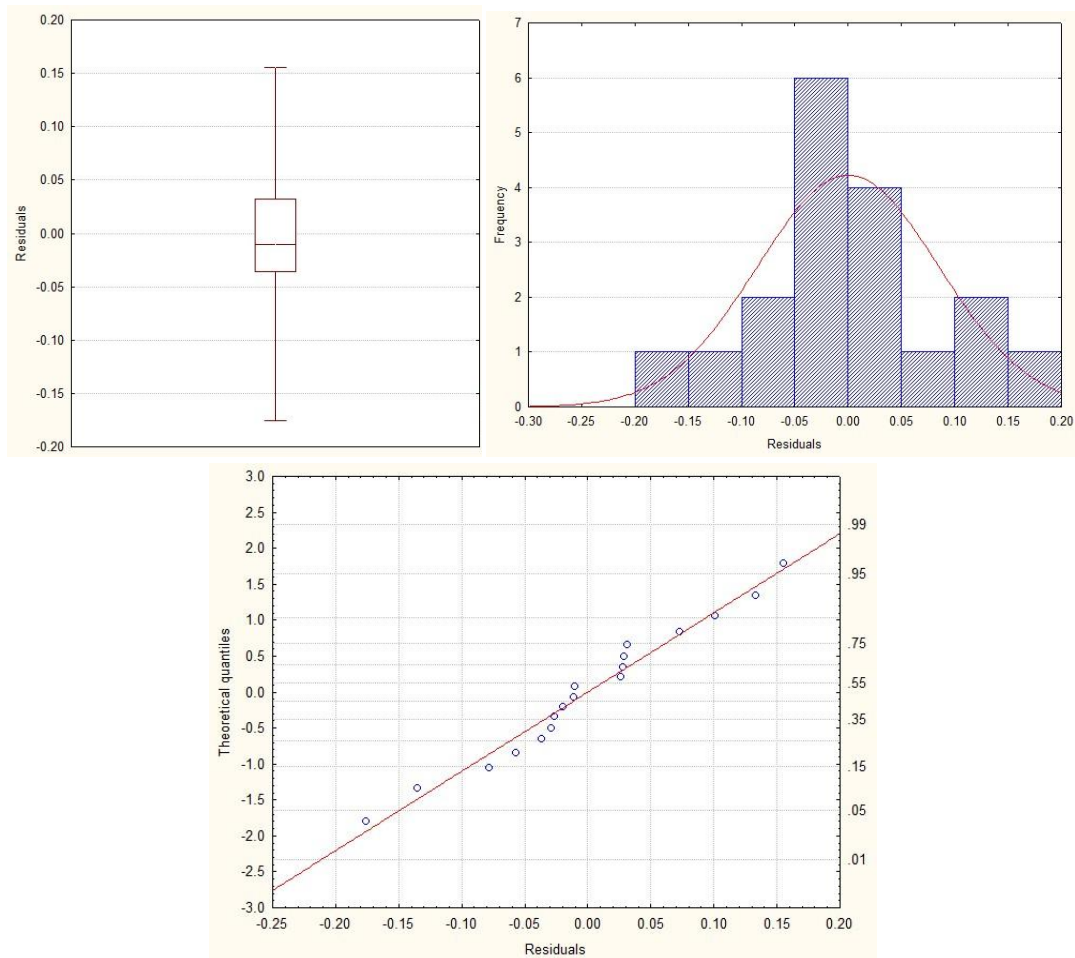


Figure 4.11 – Box plot, histograms and normal probability plot of residuals for  $\ln(\text{CS CR})$  variable

It is possible to observe that they are normally distributed. Figure 4.12 shows residuals versus observed and predicted values: points are randomly distributed around zero and no particular pattern is evident.

The same conclusions may be drawn by the residuals versus case number plot (see Figure 4.13). Moreover the lack of randomization could have cause interdependence of residuals, which is not observed.

The goodness of fit of the estimated model can be seen also in Figure 4.14, where predicted values are plotted versus the observed ones.

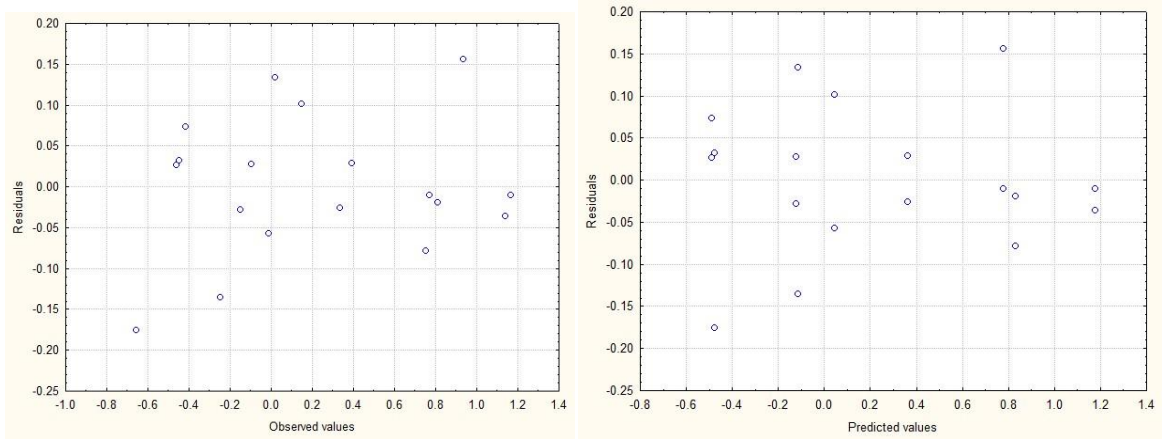


Figure 4.12 – Residuals vs. observed (left) and predicted (right) values

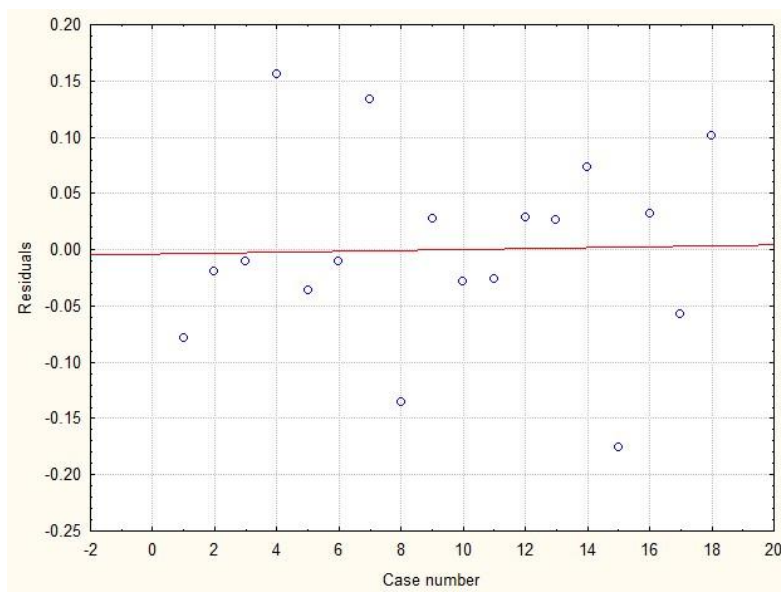


Figure 4.13 – Residuals vs. case number



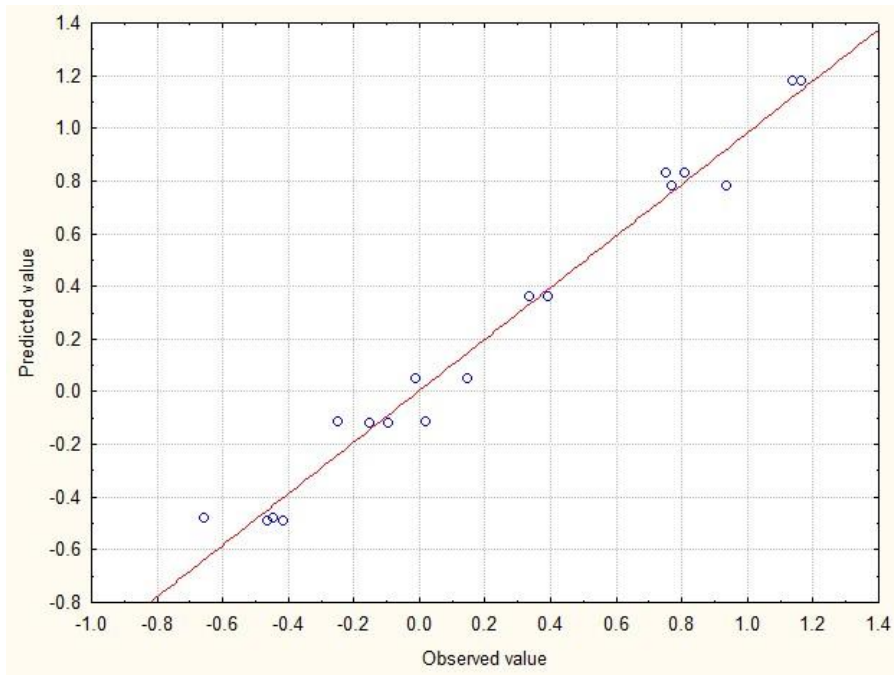


Figure 4.14 – Predicted vs. observed vlues for  $\ln(\text{CS CR})$

### Response surface

Figure 4.15 and Figure 4.16 show the response surface and the contour plot for the transformed variable (i.e.  $\ln\text{CR}$ ), whereas Table 4.8 reports the calculated coefficients for the considered effects.

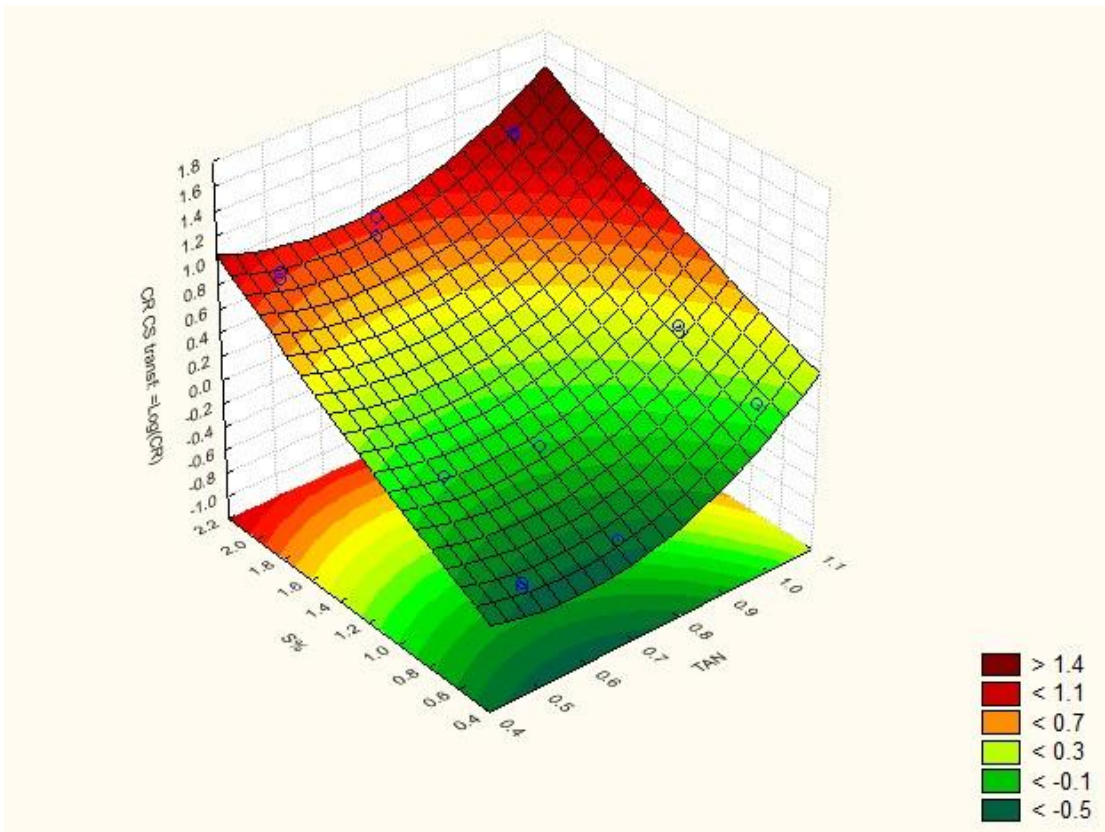


Figure 4.15 – Response surface for  $\ln(\text{CS CR})$

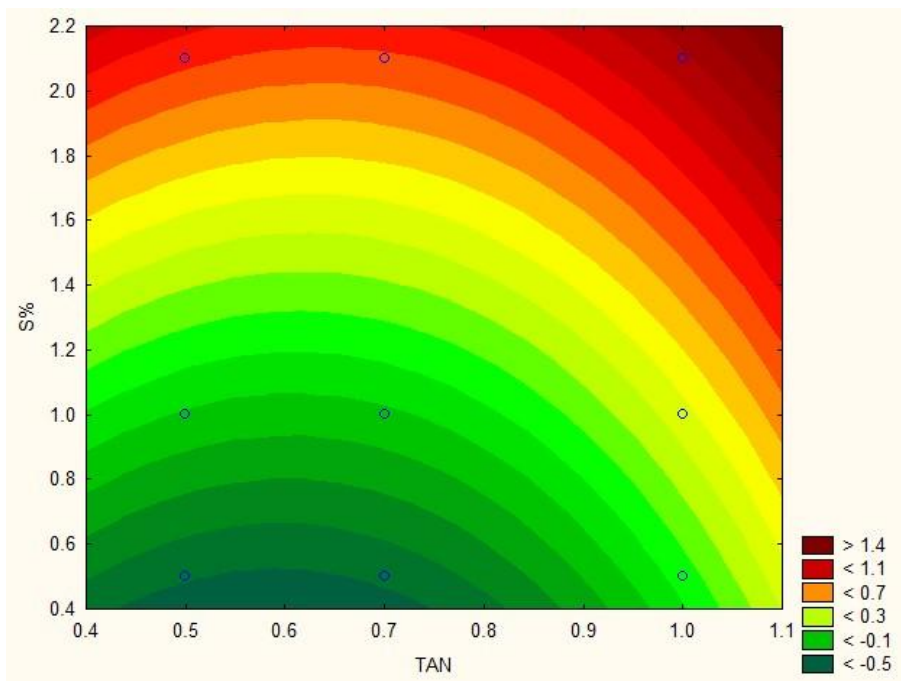


Figure 4.16 – Contour plot for  $\ln(\text{CS CR})$

Table 4.8 – Coefficients of the model for  $\ln(\text{CS CR})$ 

	<b>Regress. (Coeff.)</b>	<b>Std. Err.</b>	<b>t(12)</b>	<b>p</b>	<b>-95.% (Cnf.Lim.)</b>	<b>+95.% (Cnf.Lim.)</b>
<b>Mean/Interc.</b>	0.31335	0.485065	0.64599	0.530446	-0.74352	1.37021
<b>(1)TAN (L)</b>	-4.02348	1.291928	-3.11433	0.008949	-6.83835	-1.20861
<b>TAN (Q)</b>	3.47495	0.859841	4.04139	0.001635	1.60152	5.34838
<b>(2)S% (L)</b>	0.68774	0.263409	2.61093	0.022762	0.11382	1.26166
<b>S% (Q)</b>	0.06770	0.094124	0.71928	0.485743	-0.13738	0.27278
<b>1Q x 2L</b>	-0.15734	0.114116	-1.3788	0.193126	-0.40598	0.09130

It is possible to observe that both NAs and sulphur contribute to the environment aggressiveness, however, sulphur shows the strongest effect. On the other hand acidity appears to affect the corrosivity more at high concentration levels.

#### 4.3.2. 5Cr steel analysis of data

Figure 4.17 shows different plots of corrosion rate of 5Cr steel. Data appear to have a quite good normal distribution.

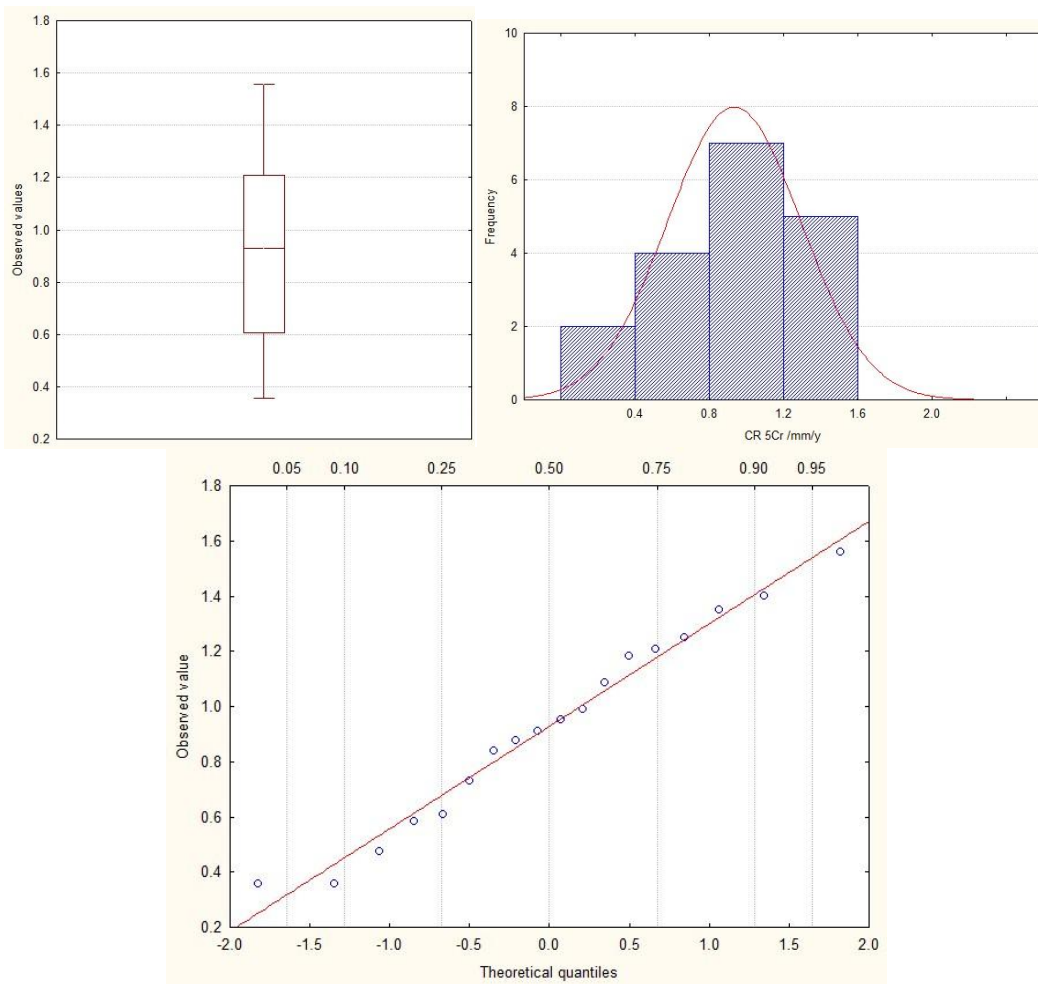


Figure 4.17 – Box-plot, histograms and normal probability plot for 5Cr CR

Figure 4.18 reports box-plot for each factor. It is possible to observe that, as expected, both factors affect corrosion rate, in particular sulphur can both increase or reduce the aggressiveness of the environment.

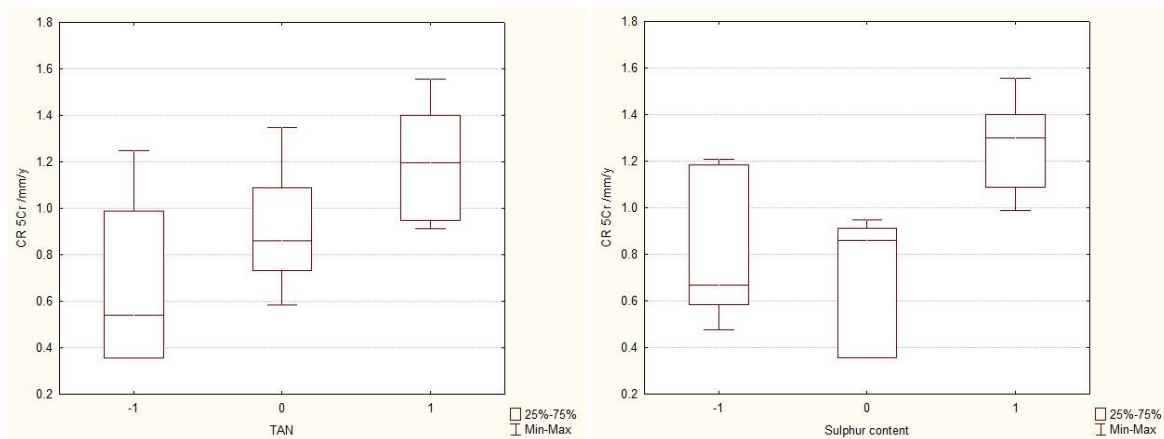


Figure 4.18 – Box-plot of response variable for TAN (left) and Sulphur (right)

### Theoretical model

The ANOVA table for the complete model is reported in Table 4.9.

Table 4.9 – ANOVA table of the complete model for 5Cr CR

	SS	DF	MS	F	p
<b>(1)TAN (L)</b>	0.764884	1	0.764884	67.44927	0.000018
<b>TAN (Q)</b>	0.004470	1	0.004470	0.39422	0.545691
<b>(2)S% (L)</b>	0.642334	1	0.642334	56.64260	0.000036
<b>S% (Q)</b>	0.202052	1	0.202052	17.81742	0.002236
<b>1L x 2L</b>	0.043557	1	0.043557	3.84094	0.081667
<b>1L x 2Q</b>	0.000091	1	0.000091	0.00807	0.930407
<b>1Q x 2L</b>	0.006759	1	0.006759	0.59603	0.459886
<b>1Q x 2Q</b>	0.124959	1	0.124959	11.01921	0.008947
<b>Error</b>	0.102061	9	0.011340		
<b>Total SS</b>	2.202407	17			

This fit has an  $R^2$  of 0.95366 and an adjusted  $R^2$  of 0.912. If we consider p-values, i.e. statistical significance, however not all interactions are actually important in the model.

Hence it is possible to simplify the model and eliminate some useless terms. Third order interaction terms are therefore discarded, whereas TAN quadratic term is kept, because it is a main effect.

The consequent ANOVA table is reported in Table 4.10.

Table 4.10 – ANOVA table of the simplified model for 5Cr CR

	<b>SS</b>	<b>DF</b>	<b>MS</b>	<b>F</b>	<b>p</b>
<b>(1)TAN (L)</b>	0.762964	1	0.762964	77.08291	0.000003
<b>TAN (Q)</b>	0.003031	1	0.003031	0.30622	0.591078
<b>(2)S% (L)</b>	0.641140	1	0.641140	64.77494	0.000006
<b>S% (Q)</b>	0.204104	1	0.204104	20.62079	0.000842
<b>1L x 2L</b>	0.051181	1	0.051181	5.17086	0.044001
<b>1Q x 2Q</b>	0.119173	1	0.119173	12.04018	0.005241
<b>Error</b>	0.108878	11	0.009898		
<b>Total SS</b>	2.202407	17			

At this stage the model appears to account for the most of the variability in the response with an adjusted  $R^2$  of 0.924.

### Residual analysis

The distribution of the residuals can be studied in different ways by quantile-quantile, box and histogram plots (see Figure 4.19). It can be seen that residuals have a quite normal distribution even if there are “fat” tails. However this can be attributed to the sample dimension, which is not so high.

Figure 4.20 shows the residual vs. observed and predicted values: there is no particular pattern and residuals appear to be randomly distributed around zero, i.e. the model doesn't over- or underestimate corrosion in correspondence of particular values.

Looking at the residual versus case number plot (see Figure 4.21), it is possible to say that there is no correlation.

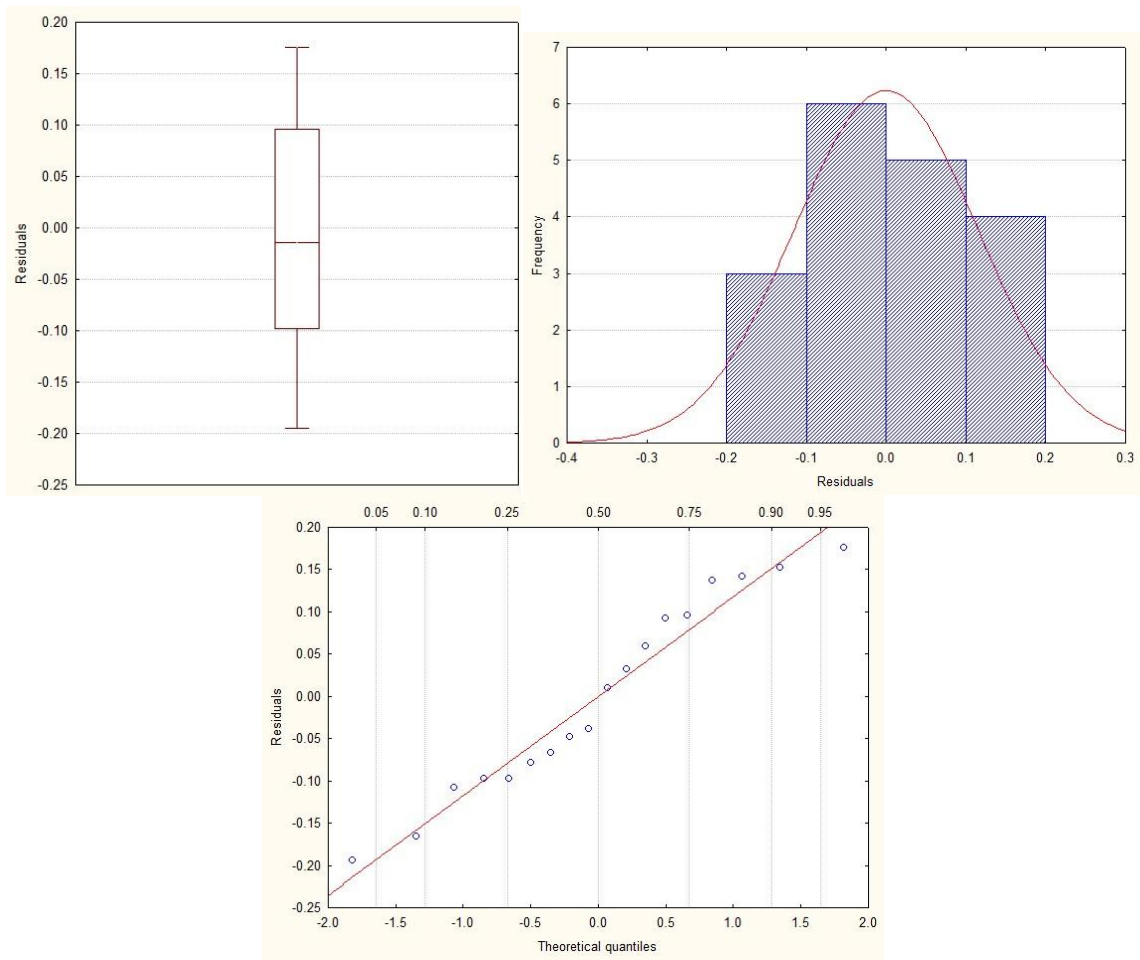


Figure 4.19 – Box-plot, histograms and normal probability plot of residuals for 5Cr CR

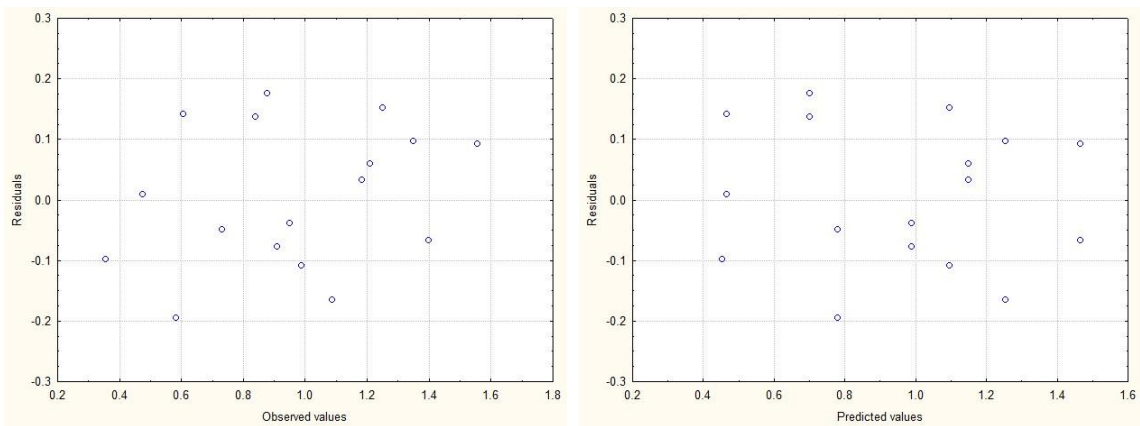


Figure 4.20 – Residuals vs. observed (left) and predicted values (right)

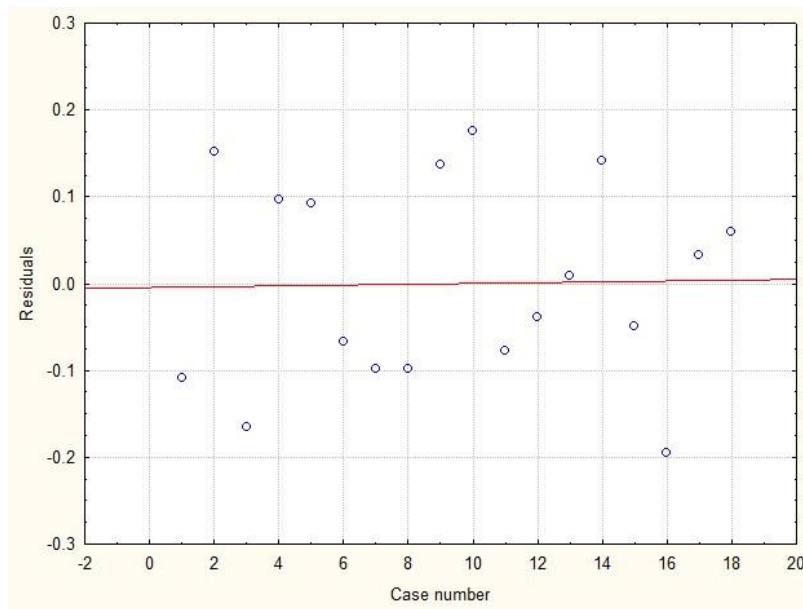


Figure 4.21 – Residuals vs. case number

Figure 4.22 shows the model response surface and Figure 4.23 the contour plot.

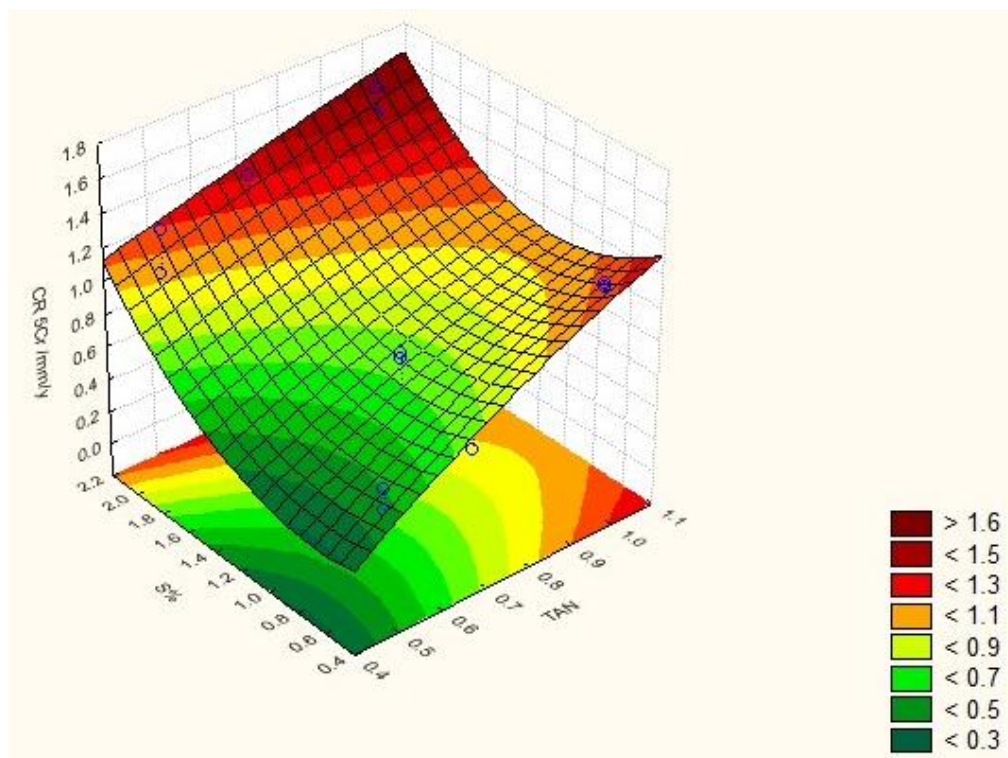


Figure 4.22 – Response surface for 5Cr CR



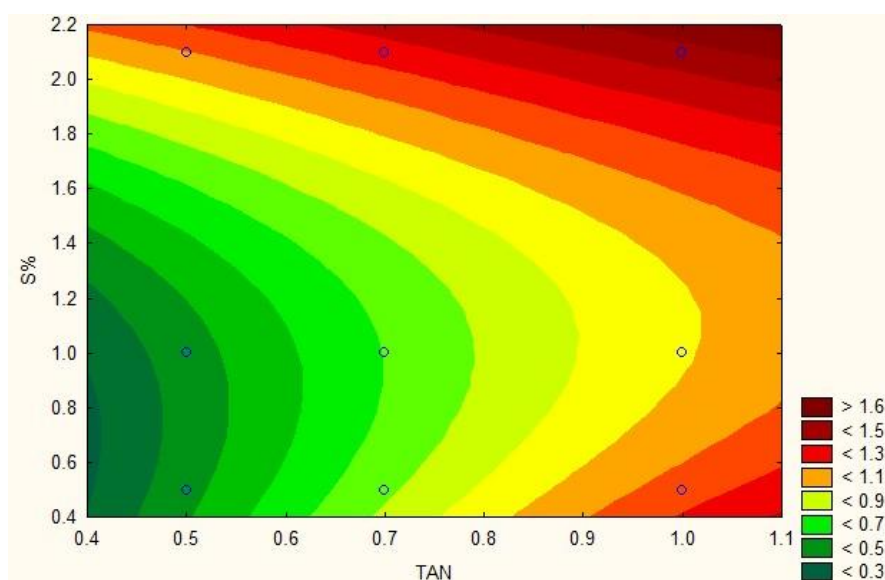


Figure 4.23 – Contour plot for 5Cr CR

The diagrams show clearly that corrosion rate increases both with sulphur content and acidity, however, there is a sulphur content that minimises environment aggressiveness and this effect is more marked at high TAN values.

Calculated coefficients are reported in Table 4.11.

Table 4.11 –Coefficients of the model for 5Cr CR

	Regress. (Coeff.)	Std. Err.	t(11)	p	-95.% (Cnf.Lim.)	+95.% (Cnf.Lim.)
<b>Mean/Interc.</b>	-0.559	1.141	-0.490	0.633	-3.071	1.952
<b>(1)TAN (L)</b>	2.799	2.550	1.097	0.295	-2.814	8.414
<b>TAN (Q)</b>	-0.693	1.379	-0.502	0.625	-3.730	2.343
<b>(2)S% (L)</b>	-0.155	1.145	-0.135	0.894	-2.676	2.365
<b>S% (Q)</b>	0.348	0.247	1.410	0.186	-0.195	0.893
<b>1L x 2L</b>	-0.873608	1.482198	-0.589	0.567	-4.135	2.388
<b>1Q x 2Q</b>	0.122886	0.359532	0.341	0.738	-0.668	0.914

#### 4.4. Tests with natural acidic crude oils

Further tests were carried out with crude F and a blend of crudes B and D (see Table 2.7), in the same temperature and flow conditions as the experimental plan. Test matrix and results are reported in Table 4.12.

Table 4.12 – Test matrix and results for acid crudes

Crude	S%	TAN	CR CS /mm/y	CR 5Cr /mm/y
<b>25%B + 75%D</b>	2.5	0.85	2.49	2.04
<b>F</b>	0.36	0.85	2.32	1.60

Results show that corrosion rates of the blend are in agreement with the data of the experimental plan, whereas crude F causes very high corrosions above all on carbon steel.

Figure 4.24 shows the surface appearance of 5Cr steel: by comparing the two images it is possible to observe that the iron/chromium sulphide layer exhibits two distinct morphologies. In fact, there is an upper cracked layer and an underneath compact layer, whose presence is revealed only after pickling when the corroded surface of the bare metal is exposed.

Figure 4.25 shows the surface appearance of carbon steel. In this case the iron sulphide layer is almost not present and the pickled surface reveals the presence of localised attack.

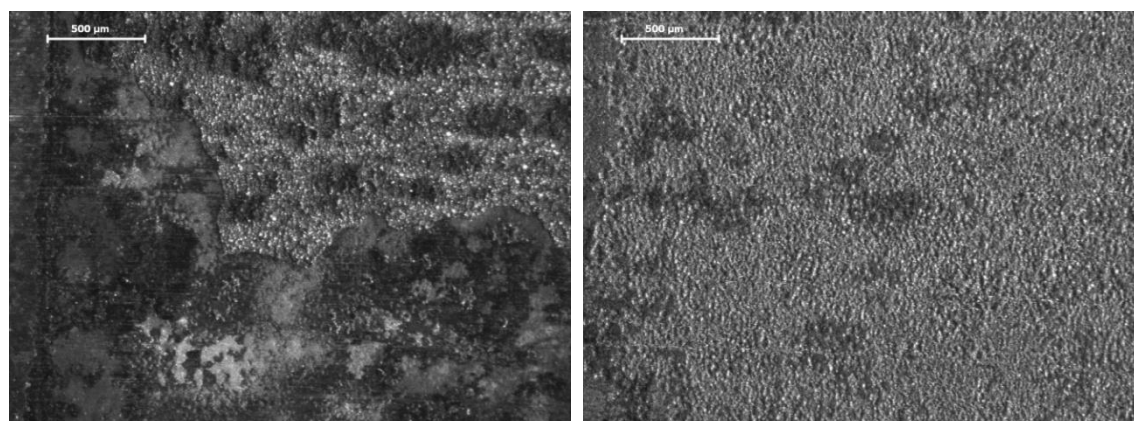


Figure 4.24 – Surface appearance of 5Cr steel coupon after the test (left) and then after pickling (right)

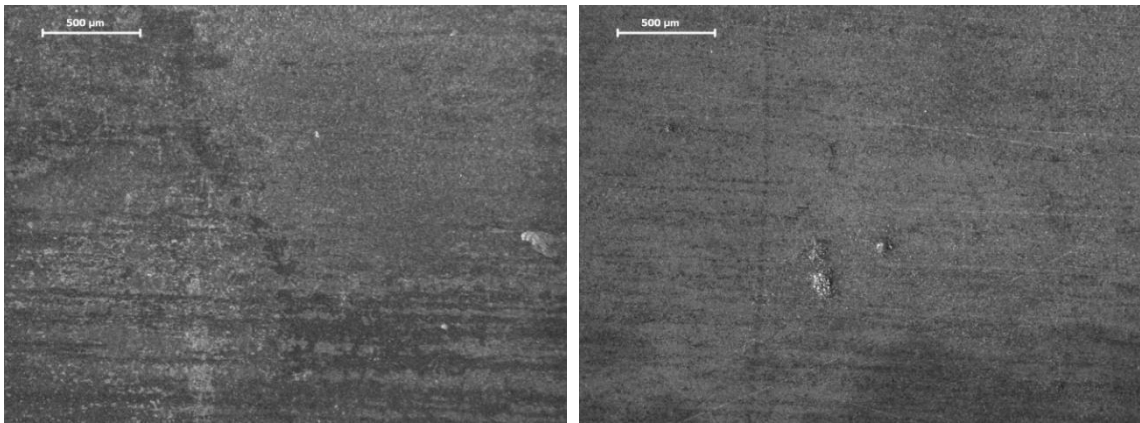


Figure 4.25 – Surface appearance of CS coupon after the test (left) and then after pickling (right)

#### 4.5. Discussion

Corrosion rate values in the presence of sulphur are generally quite high especially concerning 5Cr steel. In fact, this alloy is used right to prevent high temperature sulphidation and obtained data are not congruent with this practice.

On the other hand, considering results obtained in gasoil and naphthenic acids, a TAN value of 4, which is quite high, is needed to cause corrosion rates above 0.5 mm/y. Similarly corrosion rates at 2.1%S and 0.5 TAN (Case n.1 and 2) are comparable to the ones obtained in crude D without NAs addiction.

Although corrosion rates determined after three days may be affected by the high corrosivity occurring during the first day of test, the plant seems to amplify high temperature sulphidation.

Since a continuous layer of FeS was never detected on specimens, we can suppose that flow dynamic conditions are too severe to allow the growth of a stable layer of protective corrosion products. Or else not enough H<sub>2</sub>S is available because the decomposition of sulphur compounds to produce hydrogen sulphide is restrained by the short residence time at high temperature. This hypothesis can be substantiated by the fact that no pressure increase was recorded during any of the tests. As a consequence the H<sub>2</sub>S that is evolved is rapidly consumed by the reaction with iron, but the newly formed FeS is then carried away by the high flow velocity.

Nonetheless, data from experimental plan show that 5Cr corrosion behaviour exhibits two boundaries, depending on sulphur content: the first is between NA dominated and sulphur mitigated corrosion, then between the latter and high temperature sulphidation (see Figure 4.26).

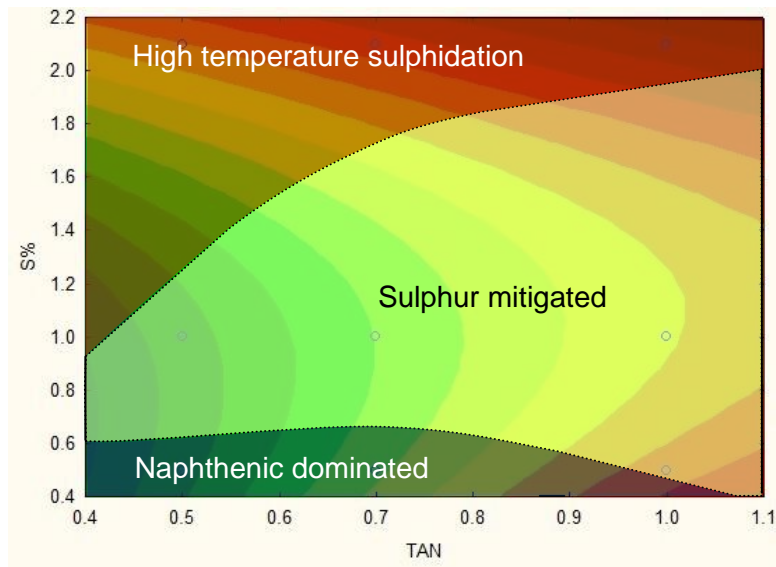


Figure 4.26 – Corrosion mechanisms and environment composition for 5Cr steel

Considering carbon steel (see Figure 4.27) we observe that there is a threshold TAN value above which corrosion rate increases sharply with acid concentration, marking a kind of transition from sulphidation to naphthenic acid dominated regime. This transition should be a function of the total sulphur content<sup>57</sup> but we observe only a weak dependence: this is consistent with the absence of iron sulphide protective layer due to high shear stresses and not enough H<sub>2</sub>S evolution.

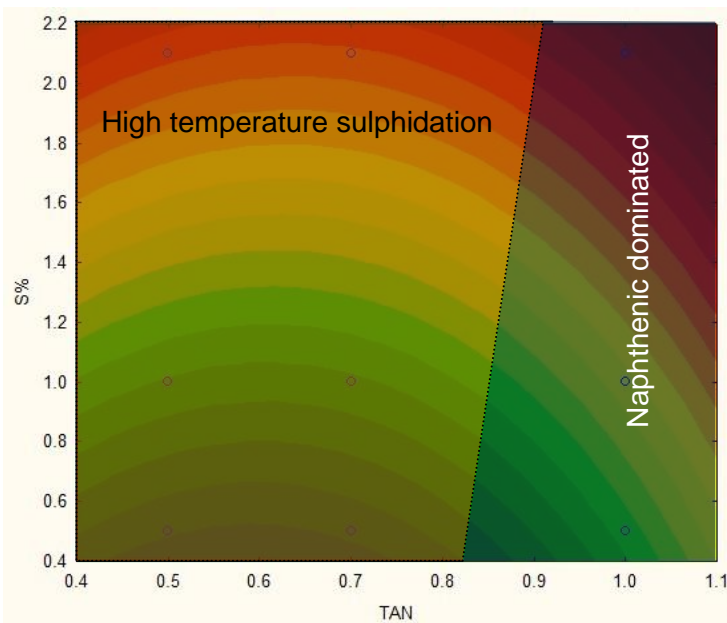


Figure 4.27 – Corrosion mechanisms and environment composition for CS

Results from tests with naturally acid crude F show that its acid compounds seem to be more aggressive despite the higher carbon number and this can be related to the presence of molecules mainly without rings (see Figure 4.28), hence easily adsorbable on the metal surface. Moreover, a different sulphide layer is produced on 5Cr steel which appears to be to some extent protected by it, despite the low sulphur content.

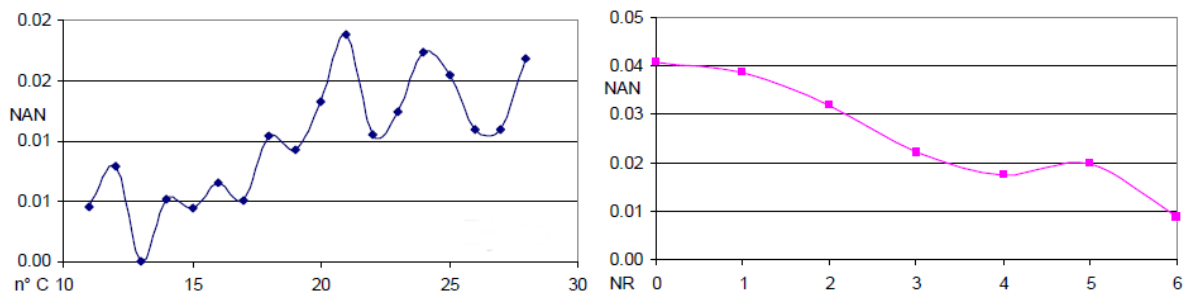


Figure 4.28 – NA distribution in crude F vs. number of C atoms (left) and of rings(right)



## Conclusions and future perspectives

The optimisation of an analytical protocol allowed to determine the main molecular characteristics of the acids present both in standard mixture and in crude oils. The procedure comprises the analysis by NMR and FTIR spectroscopy and extraction with subsequent HPLC-ESI-MS. These techniques allow to quantify the acidity due to carboxylic groups, to assess how these are bonded to the molecules and to determine the number of carbon atoms and rings.

The preliminary experimental activity was conducted in conventional autoclaves. The HP-HT experimentation confirmed that both acidity and content of sulphur species affect the crude oil aggressiveness, but the degree of interaction strongly depends on the material and on the extent of H<sub>2</sub>S evolution. A first attempt was made to separate the contribution of sulphidation and NA attack to corrosion.

A new concept testing system was developed to assess crude oil corrosivity which allows to control temperature and pressure parameters just in the vicinity of the studied specimen. The system design avoids the degradation of the testing fluid, hence the concentration of aggressive species does not change during the test. The special coupon holder allows high velocities on the surface of specimens. By adjusting the various control parameters it is possible to reproduce the conditions of different plant sections.

It was demonstrated that low alloyed steels seem to be affected by severe high temperature sulphidation caused by a synergic effect of high velocity together with

---

the difficulty in forming a protective layer of iron and chromium sulphide, due to low H<sub>2</sub>S evolution. A preliminary comparison between results obtained with a commercial mixture of NA and with crudes containing different acid compounds is in agreement with the literature where it is reported that corrosivity seems to be related to the dimension and the number of rings of the naphthenic acid molecule. However, to find a more accurate correlation between corrosivity and oil composition, further tests with different acidic crudes are needed.





## References

1. Clemente, J.; Fedorak, P.; A review of the occurrence, analyses, toxicity, and biodegradation of naphthenic acids. *Chemosphere*, vol. 60, n. 5, pp. 585-600, 2005.
2. Brient, J.; Wessner, P.; Doyle, M.; Naphthenic Acids. in *4th ed. Kirk-Othmer encyclopedia of chemical technology*, New York, John Wiley and Sons, 1995, pp. 1017-1029.
3. *ASTM Standard D664, Standard test method for acid number of petroleum products by potentiometric titration*, West Conshohocken, PA: ASTM International, [www.astm.org](http://www.astm.org).
4. *ASTM Standard D974, Standard test method for acid and base number by color-indicator titration*, West Conshohocken, PA: ASTM International, [www.astm.org](http://www.astm.org).
5. Tomczyk, N.; Winans, R.; Shinn, J.; Robinson, R.; On the nature and origin of acidic species in petroleum. 1. Detailed acidic type distribution in a California crude oil. *Energy and Fuels*, vol. 15, n. 6, pp. 1498-1504, 2001.
6. Slavcheva, E.; Shone, B.; Turnbull, A.; Review of naphthenic acid corrosion in oilrefining. *British Corrosion Journal*, vol. 34, n. 2, pp. 125-131, 1999.
7. Clemente, J.; Prasad, N.; McKinnon, M.; Fedorak, P.; A statistical comparison of naphthenic acids characterized by gas chromatography mass spectrometry. *Chemosphere*, vol. 50, n. 10, pp. 1265-1274, 2003.
8. Hsu, C.; Dechert, G.; Robbins, W.; Fukuda, E.; Naphthenic acids in crude oils characterized by mass spectrometry. *Energy & Fuels*, vol. 14, n. 1, pp. 217-223, 2000.
9. Rudzinski, W.; Oehlers, L.; Zhag, Y.; Najera, B.; Tandem mass spectrometric characterization of commercial naphthenic acid and a Maya crude oil. *Energy & Fuels*, vol. 16, pp. 1178-1185, 2002.
10. Havre, T.; Formation of calcium naphthenate in water/oil systems, naphthenic acid chemistry and emulsion stability. Ph.D. dissertation, Norwegian University of Science and Technology, Trondheim, Dept. of Chemical Engineering, 2002.
11. Håvåg, S.; Qualitative and quantitative determination of naphthenic acids in Heidrun crude oil. Master thesis, University of Oslo, Faculty of mathematics and natural sciences, Dept. of Chemistry, 2006.
12. Bataineh, M.; Scott, A.; Fedorak, P.; Martin, J.; Capillary HPLC/QTOF-MS for characterizing complex naphthenic acid mixtures and their microbial transformation. *Analytical Chemistry*, vol. 78, pp. 8354-8361, 2006.

13. Alvisi, P.; Lins, V.; An overview of naphthenic acid corrosion in avacuum distillation plant. *Engineering Failure Analysis*, vol. 18, pp. 1403-1406, 2011.
14. Piehl, R.; Naphthenic acid corrosion in crude distillation units, in *NACE International Corrosion Conference*, Paper n.196, 1987.
15. Wu, X.; Jing, H.; Zheng, Y.; Yao, Z.; Ke, W.; Resistance of Mo bearing stainless steels and Mo-bearing stainless steel coating to naphthenic acid corrosion and erosion- corrosion. *Corrosion Science*, vol. 46, pp. 1013-1032, 2004.
16. Qu, D.; Zheng, Y.; Jing, H.; Yao, Z.; Ke, W.; High temperature naphthenic acid corrosion and sulphidic corrosion of Q235 and 5Cr1/2/Mo steels in synthetic refining media. *Corrosion Science*, vol. 48, pp. 1960-1985, 2006.
17. Tebbal, S.; Kane, R.D.; Review of critical factors affecting crude corrosivity. in *NACE International Corrosion Conference*, Paper n. 607, 1996.
18. Tebbal, S.; Schutt, H.; Podlecki, R.; Sudhakar, C.; Analysis and Corrosivity Testing of eight crude oils. in *NACE International Corrosion Conference*, Paper n. 636, 2004.
19. Groysman, A.; Brodsky, N.; Penner, J.; Goldis, A.; Savchenko, N.; Study of corrosiveness of acidic crude oil and its fractions. in *NACE International Corrosion Conference*, Paper n.568, 2005.
20. Laredo, G.; López; Álvarez, R.; Castillo, J.; Cano, J.; Identification of naphthenic acids and other corrosivity-related characteristics in crude oil and vacuum gas oils from a mexican refinery. *Energy & Fuels*, vol. 18, n. 6, pp. 1687-1694, 2004.
21. Hau, J.; Yépez, O.; Torres, L.; Specht, M.; Classifying crude oils according to corrosivity using the iron powder test. in *NACE International Corrosion Conference*, Paper n. 699, 2000.
22. Laredo, G.; López; Álvarez, R.; Cano, J.; Naphthenic acids, total acid number and sulfur content profile characterization in Isthmus and Maya crude oils. *Fuel*, vol. 83, pp. 1689-1695, 2004.
23. Groysman, A.; Brodsky, N.; Penner, J.; Shmulevich, D.; Skorodinsky, S.; Naphthenic acid corrosion study. in *Eurocorr 2007, Conference Proceedings*, 2007.
24. Smart, N.; Rance, A.; Pritchard, A.; Laboratory investigation of naphthenic acid corrosion under flowing conditions. in *NACE International Corrosion Conference*, Paper n. 484, 2002.
25. Gabetta, G.; Mancini, N.; Montanari, L.; Oddo, G.; Preliminary results of a project on crude oil corrosion. in *NACE International Corrosion Conference*, Paper n. 644, 2003.

- 
26. Qu, D.; Zheng, Y.; Jiang, X.; Ke, W.; Correlation between the corrosivity of naphthenic acids and their chemical structures. *Anti-Corrosion Methods and Materials*, vol. 54, n. 4, pp. 211-218, 2007.
  27. Slavcheva, E.; Shone, B.; Turnbull, A.; Factors controlling naphthenic acid corrosion. in *NACE International Corrosion conference*, Paper n. 579, 1998.
  28. Messer, B.; Tarleton, B.; Beaton, M.; Phillips, T.; New theory for naphthenic acid corrosivity of Athabasca oilsands crudes. in *NACE International Corrosion Conference*, Paper n. 634, 2004.
  29. Messer, B.; Tarleton, B.; Beaton, M.; Compositions, configurations, and methods of reducing naphthenic acid corrosivity, International Patent WO 040313 A1 (2005), US 0164137 A1 (2008)».
  30. Piehl, R.; Naphtenic acid corrosion in crude distillation units. *Material Performance*, vol. 27, no. 1, pp. 37-43, 1988.
  31. Babaian-Kibala, E.; Craig, H.; Rusk, G.; Quinter, R.; Summers, M.; Naphthenic Acid Corrosion in Refinery Settings. *Material Performance*, pp. 50-55, 1993.
  32. Jayaraman, A.; Saxena, R.C.; Corrosion and its control in petroleum refineries - A review. *Corrosion Prevention & Control*, vol. 42, n. 6, pp. 123-131, 1995.
  33. Babaian-Kibala, E.; Craig, H.; Rusk, G.; Blanchard, K.; Rose, T.; Uehlein, B.; Quinter, R.; Summers, M.; Naphthenic acid corrosion in a refinery setting. in *NACE International Corrosion Conference*, Paper n. 631, 1993.
  34. Bota, G.; Qu, D.; Nestic, S.; Wolf, H.; Naphthenic acid corrosion of mild steel in the presence of sulfide scales formed in crude oil fractions at high temperature. in *NACE International corrosion conference*, Paper n.353, 2010.
  35. Cayard, R.; Kane, M.; A comprehensive study on naphthenic acid corrosion. in *NACE International Corrosion Conference*, Paper n. 555, 2002.
  36. Yépez, O.; Influence of different sulfur compounds on corrosion due to naphthenic acid. *Fuel*, vol. 84, pp. 97-104, 2005.
  37. Wu, X.; Jing, H.; Zheng, Y.; Yao, Z.; Ke, W.; Erosion-corrosion of various oil-refining materials in naphthenic acid. *Wear*, vol. 256, pp. 133-144, 2004.
  38. Craig, H.; Temperature and velocity effects in naphthenic acid corrosion. in *NACE International corrosion conference*, Paper n.603, 1996.
  39. Trasatti, S.P.M.; Gabetta, G.; Naphthenic acid corrosion of carbon steels by neural network and autoclave testing. in *Eurocorr 2005, Conference Proceedings*, 2005.
  40. Gallo, G.; Edmondson, J.; The effect of molybdenum on stainless steels and naphthenic acid corrosion resistance. in *NACE International Corrosion Conference*, Paper n. 555, 2008.

41. Barrow, M.; McDonnell, L.; Feng, X.; Walker, J.; Derrick, P.; Determination of the Nature of Naphthenic Acids Present in Crude Oils Using Nanospray Fourier Transform Ion Cyclotron Resonance Mass Spectrometry: The Continued Battle Against Corrosion. *Analytical Chemistry*, vol. 75, n. 4, 2003.
42. Hur, M.; Yeo, I.; Kim, E.; No, M.; Koh, J.; Cho, Y.; Lee, J.; Kim, S.; Correlation of FT-ICR Mass Spectra with the Chemical and Physical Properties of Associated Crude Oils. *Energy & Fuels*, vol. 24, p. 5524–5532, 2010.
43. Headley, J.; Peru, K.; Barrow, M.; Mass spectrometric characterization of naphthenic acids in environmental samples: a review. *Mass Spectrometry Reviews*, vol. 28, p. 121– 134, 2009.
44. Ali, F.; Hameed Khan, Z.; Ghaloum, N.; Structural Studies of Vacuum Gas Oil Distillate Fractions of Kuwaiti Crude Oil by Nuclear Magnetic Resonance. *Energy & Fuels*, vol. 18, pp. 1798-1805, 2004.
45. Rikka, P.; Spectrometric identification of naphthenic acids isolated from crude oil, Master thesis, Texas State University, Dept. of Chemistry and Biochemistry, San Marcos, TX, 2007.
46. Hau, J.; Yépez, O.; Specht, M.; Lorenzo, R.; The iron powder test for naphthenic acid corrosion studies. in *NACE International Corrosion Conference*, Paper n. 379, 1999.
47. Yépez, O.; Method for determining the corrosiveness of naphthenic acid in crude oil and refinery streams. European Patent Application 1039290 A2, 2000.
48. Yépez, O.; Method for determining the corrosiveness of naphthenic acid in crude oil refinery streams. United States Patent 6,294,387 B1, 1999.
49. Groysman, A.; Brodsky, N.; Penner, J.; Goldis, A.; Savchenko, N.; Study of corrosiveness of acidic crude oil and its fractions. in *Eurocorr The European Corrosion Congress, Conference proceedings*, 2005.
50. De Jong, J.; Dowling, N.; Sargent, M.; Etheridge, A.; Saunders-Tack, A.; Fort, W.; Effect of Mercaptans and other organic sulfur species on high temperature corrosion in crude and condensate distillation units. in *NACE International Corrosion Conference*, Paper n. 565, 2007.
51. *ASTM Standard G31, Standard Guide for Laboratory Immersion Corrosion Testing of Metals*, West Conshohocken, PA: ASTM International, [www.astm.org](http://www.astm.org).
52. *NACE Standard TM0169, Standard Test Method - Laboratory Corrosion Testing of Metals*, Houston, TX: NACE International.
53. Pritchard, A., Graham, Rance, A.; Use of a rotating cylinder system to determine the corrosivities of acid crudes. in *NACE International Corrosion*

- 
- Conference*, paper n. 525, 2001.
54. Wu, X.; Jing, H.; Zheng, Y.; Yao, Z.; Ke, W.; Corrosion and erosion-corrosion behaviors of carbon steel in naphthenic acid media. *Materials and Corrosion*, vol. 53, pp. 833-844, 2002.
  55. Davies, O.L.; *The design and analysis of industrial experiments*, New York: Longman Inc., 1956.
  56. NACE International Publication 34103, *Overview of Sulfidic Corrosion In Petroleum Refining*, NACE International, Houston, TX, 2004.
  57. Kanukuntla, V.; Qu, D.; Nescic, S.; Experimental study of concurrent naphthenic acid and sulfidation corrosion. in *17th International Corrosion Congress*, Paper n.2764, 2009.